Influence of Contact Conditions on Thermal Responses of the Hand

by

Jessica Anne Galie

B.S. Mechanical Engineering
University of Maryland, 2004

Submitted to the Department of Mechanical Engineering
in partial fulfillment of the requirements for the degree of

Master of Science in Mechanical Engineering

at the

Massachusetts Institute of Technology

March 2009

Signature of Author: _____
Department of Mechanical Engineering
March 5, 2009

Certified by: _____
Lynette A. Jones
Principal Research Scientist in Mechanical Engineering
Thesis Supervisor

Accepted by: _____
David E. Hardt
Chairman, Department Committee on Graduate Students

Influence of Contact Conditions on Thermal Responses of the Hand

by

Jessica Anne Galie

Submitted to the Department of Mechanical Engineering
on March 5, 2009 in partial fulfillment of the
requirements for the degree of Master of Science in
Mechanical Engineering

Abstract

The objective of the research conducted for this thesis was to evaluate the influence of contact conditions on the thermal responses of the finger pad and their perceptual effects. A series of experiments investigated the thermal and perceptual effects of different contact conditions including contact force, contact duration, the object's surface temperature, and its surface roughness. The thermal response of the finger pad was measured using an infrared camera as the contact force varied from 0.1 to 6 N. It was determined that the decrease in skin temperature was highly dependent on the magnitude of contact force as well as contact duration. A second set of experiments investigated the effect of surface texture on the thermal response of the finger pad, and demonstrated, contrary to predictions, that a greater change in skin temperature occurs when the finger is in contact with rougher surfaces. The effect of varying surface texture on the perception of temperature was also investigated. The changes in temperature due to varying surface texture are perceptible, and demonstrate that the perception of surface roughness is not only influenced by changes in temperature, but in turn affects the perception of temperature. The final set of experiments examined the effect of varying the surface temperature of the thermal display on the perceived magnitude of finger force. Over the range of 20 to 38 °C, the surface temperature of the display did not have a significant effect on the perceived magnitude of force. The results of these experiments can be incorporated into thermal models that are used to create more realistic displays for virtual environments and teleoperated systems.

Thesis Supervisor: Lynette A. Jones
Title: Principal Research Scientist in Mechanical Engineering

Acknowledgments

I would like to express my sincere gratitude to my advisor, Dr. Lynette Jones, for her guidance and advice throughout the process of this research. I have learned a tremendous amount from her, and she has given me the opportunity to grow as a researcher. I would also like to thank Prof. Ian Hunter for providing a wonderful laboratory experience with numerous resources. Thank you to all of the members of the BioInstrumentation Lab, who provided useful and constructive feedback. I continue to be amazed with your willingness to help whenever needed.

I am especially grateful to my parents, Patricia and John, for their endless support in whatever I have chosen to pursue, and my Mom who bought me a book bag and folders to send me off to school again. I owe many thanks to my sisters, Gina and Terry, and my brother, Pete, for their cross-functional engineering input and encouragement. A special thanks to Mike, who has been by my side from the start of my journey at MIT until the end, and who is a constant source of motivation and inspiration to me. This thesis is dedicated to them.

This research was supported in part through the Advanced Decision Architectures Collaborative Technology Alliance sponsored by the U.S. Army Research Laboratory under Cooperative Agreement DAAD 19-01-2-0009.

Table of Contents

1 Introduction

The focus of this thesis is to evaluate how the contact conditions between the hand and an object influence the heat flux conducted out of the skin, and how these effects can be incorporated into a thermal model. Thermal cues arise from the changes in skin temperature that occur when an object is held in the hand, and assist in the identification of objects. The resting temperature of the skin is typically higher than the temperature of objects encountered in the environment, and the thermal cues used to recognize objects by touch include the rate and amplitude of the change in skin temperature. By understanding the influence of contact conditions on the thermal response of the skin, more accurate thermal models can be developed. These in turn can be implemented in thermal displays that are integrated into haptic devices so that a holistic image of a remote object in a virtual environment or teleoperated robotic system can be provided.

1.1 Haptic Sensory System

The haptic sensory system includes the tactile and proprioceptive senses, and is involved in obtaining information about and acting on objects in contact with the skin. The tactile sense refers to the sensory system that processes signals related to the mechanical properties of objects, such as surface texture and compliance, as well as their thermal characteristics. The proprioceptive sense encodes the position and orientation of limbs with the respect to the body. Both tactile and proprioceptive senses play an essential role in exploring the external environment.

The skin is the interface that interacts with an object and obtains sensory information when in contact with an object. It is the largest organ in the body, with a surface area of approximately 1.8 m^2 and mass of 4.5 to 5 kg for the average adult human (Tortora & Grabowski, 1993). There are two principal layers which comprise the skin. The epidermis is 65 to 115 μm thick, and its cells are nourished by capillaries extending from the upper layers of the dermis. The dermis is approximately 0.3 to 3 mm thick, and contains sensory nerve endings which respond to touch and pressure, temperature changes, and painful stimuli. The hypodermis is the subcutaneous tissue that is located beneath the dermis, and attaches the skin to the underlying bone and muscle and supplies it with blood vessels and nerves. The skin contains sweat glands, nerve endings, and blood vessels, which allow it to guard against bacterial infection, protect underlying muscles and organs, regulate temperature, and provide a surface for sensing and interacting with the environment.

Thousands of sensory receptors are located throughout the skin and muscle tissue. Mechanoreceptors, thermoreceptors, and nociceptors are types of sensory receptors that respond to particular stimuli. Certain parts of the body and different areas of skin are more sensitive than others, and have a higher density of receptors. Glabrous, or hairless, skin found on the hands, lips, and soles of the feet is the most sensitive to touch. (Gardner et al., 2000).

1.2 Thermal Sensation

Changes in skin temperature are encoded by cold or warm thermoreceptors, which are located in the epidermal and dermal layers of the skin. Thermoreceptors are triggered by changes in skin temperature, and transmit signals to the central nervous system that

can assist in object identification. Cold receptors are more numerous than warm receptors, and the two types of afferent units vary with respect to their conduction velocities. Cold afferent nerve fibers are faster than warm afferent fibers, with velocities in the range of 10 to 20 m/s, as compared to 1 to 2 m/s for warm afferent fibers (Darian-Smith, 1984). As the resting skin temperature is typically greater than that of objects encountered in the environment, heat flux is conducted out of the skin on contact and the cold thermoreceptors signal the decrease in skin temperature.

Thermoreceptors respond over a temperature range of 5-45 °C. Cold receptors respond to decreases in temperature from 5-43 °C, while warm receptors discharge with increases in temperature up to 45 °C (Kenshalo, 1976). Once temperatures rise above 45 °C or fall below 15-18 °C, there is a sensation of pain which is sensed by nociceptors, or pain receptors (Darian-Smith & Johnson, 1977; Harrison & Davis, 1999). Both warm and cold receptors fire spontaneously when the skin is in the thermally neutral zone between 30-36 °C, but there is no thermal sensation for areas of skin up to approximately 1500 mm^2. However, the thermal neutral zone is smaller when larger areas of skin change in temperature (Kenshalo, 1976). Outside of the thermal neutral zone, thermal sensation is typically triggered by activity in one type of receptor.

Perceiving a variation in temperature depends on several factors including the amplitude and rate of temperature change, the initial temperature of skin, and the area of the body site stimulated. On the thenar eminence at the base of the thumb, it is possible to perceive a temperature difference of 0.02-0.07 °C between two cooling pulses, and 0.03-0.09 °C between two warming pulses (Johnson et al., 1973; Johnson et al., 1979). When the skin of the thenar eminence is maintained at 33 °C, the differential threshold

for the perception of warming is 0.20 °C at a rate of 2.1 °C/s, and for cooling is 0.11 °C at a rate of 1.9 °C/s (Stevens & Choo, 1998). If the skin temperature changes at a very slow rate of 0.5 °C/min, people do not detect the change in temperature (Stevens, 1991), but at faster rates small increases and decreases in skin temperature can be detected. When the initial temperature of the skin is maintained above 36 °C, the sensation is one of continuous warmth, and when the skin is maintained below 30 °C, continuous cold sensation is perceived.

Thermal stimulation evokes sensations of warmth or cold, but the spatial features of the stimulus such as the size and shape can not be accurately resolved. The poor spatial resolution of thermal stimuli is due to the summation of intensity over area. An increase in the area of stimulation affects the perceived intensity of the stimulus, and diminishes the ability to perceive differences within the area of stimulation. For cold stimuli, the perceived intensity of cold increases with increasing stimulation area (Greenspan & Kenshalo, 1985; Kenshalo et al., 1967; Stevens & Marks, 1979). For warm stimuli, the effect of the area of stimulation on sensory thresholds becomes less important as the degree of heating increases and approaches the pain threshold (Stevens & Marks, 1971). Spatial summation may also occur when separate areas on opposite sides of the body are thermally stimulated at the same time (Marks et al., 1976; Rozsa & Kenshalo, 1977). The thresholds for both warm and cold stimuli diminish when stimuli are presented at symmetric sites simultaneously. Yet, the threshold remains the same if two asymmetric sites are stimulated simultaneously (Hardy & Oppel, 1937; Rozsa & Kenshalo, 1977).

1.3 Development of Thermal Displays

Thermal displays are used to present thermal cues to the skin on the hand to assist in the identification of a remote object in a virtual environment or teleoperated robotic system. Peltier devices, also called thermoelectric modules (TEMs), are the most widely used thermal stimulators in thermal displays. Peltier devices operate by creating a temperature difference at the junction of two dissimilar conductors in contact by passing a DC current through the circuit. The direction of heat flowing between the substrates is dependent on the current direction, and temperature differences are generated between the substrates. The magnitude of the temperature difference and the rate of change are controlled by varying the amplitude of the current passing through the Peltier device.

The heating and cooling of thermal displays is typically controlled using a closed-loop circuit with a proportional-integral (PI) or proportional-integral-derivative (PID) control loop (Ino et al., 1993; Yamamoto et al., 2004). Contact temperature sensors such as thermocouples, thermistors, or RTDs are used to provide temperature feedback to the controller. Temperature sensors with low thermal mass and small dimensions are typically chosen for thermal displays as they reach thermal equilibrium quickly and facilitate high-frequency temperature control. A temperature sensor's stability is also an important factor to consider. The working temperature range of a thermal display is usually around 20 °C, so the sensitivity of a temperature sensor is an important factor in its selection. RTDs are typically the most accurate among RTDs, thermistors, and thermocouples, but thermistors have the best sensitivity.

Non-contact thermal measurement devices are being used to overcome some of the limitations of contact temperature sensors. Thermistors and thermocouples give

localized point measurements, and do not provide a complete image of the thermal distribution across the contact area. Infrared cameras have been used to record the temperature distribution across the finger pad which has permitted a more realistic evaluation of thermal displays (Ho & Jones, 2008). When using an infrared thermal imaging system, any objects that lie in the path between the camera and the target object must be made from materials that are infrared transmissible. Since Peltier devices do not meet this requirement, thermal imaging cameras are not used in thermal displays.

Infrared lamps and fans have been used in thermal displays to convey thermal information about the environment. The Thermopad was designed for virtual reality applications, and used infrared lamps and fans to warm and cool the user, while Peltier devices induced changes in skin temperature (Dionisio et al., 1997). Lecuyer et al. (2003) devised a system for visually-impaired people in a virtual reality environment, which used infrared lamps to convey a feeling of warmth from the sun to the user.

The applications of thermal displays typically involve conveying thermal information to the user about real or virtual objects. Thermal information can be delivered through contact methods, such as Peltier devices to convey the thermal response of touching a real or simulated material, or non-contact methods such as convection or radiation, which are usually involved in larger-scale virtual environments. MacLean and Roderick (1999) designed a platform called "Aladdin", which integrates a haptic display into a commonplace manual control device, a doorknob. The system consists of a haptic knob with a torque and thermal display. The thermal display was created in the body of the knob with a thermoelectric module, which was programmed to adjust the display surface at least 15 °F above and below ambient temperature within 30

seconds. The TEM was embedded in a thermally conductive aluminum body with a smooth heat sink on the proximal knob surface to remove heat from the hot side of the Peltier device. The knob was designed to encourage a fingertip grasp on the front, controlled surface of the thermal display. Two thermocouples were used to provide temperature feedback to the controller. One thermocouple was mounted on the heat sink side, and the other was mounted on the controlled surface to complete the feedback loop. A suggested application of this device is a smart doorknob, which identifies a person and allows for keyless entry.

Yamamoto et al. (2004) focused on the control of a thermal tactile display based on the prediction of contact temperature during the initial contact period, which is when the most rapid thermal change occurs upon contact. A contact pad consisted of a Peltier device with a grooved surface, in which a thermocouple was mounted to provide temperature feedback to a PID controller regulating the surface of the contact pad. The contact pad was installed on a radiator in which an infrared sensor was mounted to detect when the finger made contact with the pad. The sensor consisted of an infrared LED and photodiode. The initial temperature of the finger was recorded by a radiation thermometer, and fed into a thermal model in the processor. When the infrared sensor detected that contact had been made with the pad, the controller set the Peltier device to the predicted contact temperature based on the thermal model. The goal of this system was to simulate the thermal conditions that occur at the moment of contact in order to provide a realistic image of the object.

Hedin et al. (2006) developed a tactile display based on thermal input to assist blind people in identifying the presence and location of humans in the surrounding

environment. A prototype device consisted of an infrared camera mounted on top of a tactile array on a hand-held frame. The tactile display imaged the output of the infrared camera, where each pixel of the tactile display was a binary up or down cue based on the threshold of the skin temperature detected by the infrared camera. Five subjects were tested with the device, and asked to identify static features and dynamic movements at a distance of 10 feet. The results showed that the subjects who were well versed in the use of Braille were able to reliably resolve the output of the tactile display.

1.4 Thermal Models

Thermal models are used to predict the changes in skin temperature when the hand makes contact with an object. The resting temperature of the skin on the hand ranges from 25 to 36 °C (Verrillo et al., 1998), and is typically higher than the temperature of objects encountered in the environment. Transient heat conduction occurs upon contact, where heat flows from the hand to the object, and causes the skin temperature on the hand to decrease. The rate and magnitude of skin temperature decrease depends on a number of factors, including the initial temperatures, conductivity and heat capacity of the skin and the object.

Most analytical thermal models that have been created are based on the Pennes bioheat equation (1948), with the exception of a model proposed by Benali-Khoudja et al. (2003) which was developed using an electrical analogy. The bioheat equation accounts for the energy balance within the tissue of metabolic heat generation and blood perfusion with thermal diffusion.

$$\rho c \frac{dT}{dt} = \nabla(k \nabla T) + (\rho c)_b \omega_b (T_a - T) + q_m$$

where ρc is the heat capacity of the tissue, T is the temperature of the tissue, k is the thermal conductivity of the tissue, $(\rho c)_b$ is the heat capacity of blood, ω_b is perfusion rate of blood, T_a is the temperature of the arterial blood, and q_m is the metabolic heat generation. The bioheat equation describes a conduction-dominated transient heat transfer process, where the metabolic heat generation is assumed to be homogenously distributed throughout the tissue and the effect of blood perfusion is homogenous and isotropic. The bioheat equation is commonly used as the foundation for bioheat transfer due to its simplicity and accuracy with experimental results. Thermal models which use the bioheat equation predict the interaction between the skin and the object based on different assumptions and boundary conditions. In these models, the initial temperatures of the skin and contact material and the effects of blood perfusion have generally been considered.

Two thermal models of the finger were proposed for virtual reality applications by Bergamasco et al. (1997) who described the thermal contact between the finger and an object. A partial differential equation (PDE) model and an ordinary differential equation (ODE) model were created to predict the transient thermal gradient perpendicular to the surface when the finger rested in free air and when the finger made contact with an object. The PDE model for the finger in free air was based on the one-dimensional bioheat equation with the assumption that the thermal properties of the tissue were spatially uniform. The PDE model for the finger in contact with an object assumed a one-dimensional conduction scenario, where the object was assumed to be a semi-infinite body, and there was no heat exchange at the tissue boundary, which was separated by a distance from the interface. The ODE model did not consider the tissue to have uniform

thermal properties, but instead divided it into 10 layers, each with different material properties. The ODE model accounts for the heat storage within each layer and the continuum of one-dimensional heat conduction from layer to layer at interfaces for both free air and contact conditions.

Kron and Schmidt (2003) adapted Bergamasco et al.'s (1997) ODE model, and applied it to three layers of skin based on anatomical structure, which included the epidermis, dermis, and hypodermis. They developed a model that was able to predict the temperature distribution inside the fingertip when it was in free air, and also when it made contact with an object. Kron and Schmidt (2003) accounted for blood perfusion and metabolic heat generation in the dermis and hypodermis.

Yamamoto et al. (2004) implemented a model-based thermal display to simulate the thermal conditions at the initial stage of contact. In this model, the object and the skin were considered to be homogenous bodies with uniform initial temperatures. Thermal contact resistance was ignored since the model was being used solely to predict the thermal behavior at the moment of contact. When thermal resistance is zero, the temperatures of both the skin and the object become the same temperature at the moment contact occurs. The thermal display presented the predicted contact temperature, and allowed the skin to undergo the same thermal sensation as if it were touching a real object. Yamamoto et al. (2004) conducted a series of experiments to evaluate the performance of their model-based thermal display. Subjects were asked to identify simulated materials (polystyrene, wood, ceramic, and brass) based on thermal cues while touching the corresponding real materials with the other hand. The mean recognition rate was 74% which was satisfactory to show that the thermal display could present cues that

are as effective as those encountered normally for identifying the material composition of objects.

Citerin et al. (2006) implemented a finite element thermal model to overcome the limitations of their analytical model, which did not account for the complex structure of the finger pad and the thermal resistance between the finger and the contact material. Both the analytical and finite element models were used to predict the temperature changes during different stages of contact, and superimposed to achieve an overall change in temperature for the entire contact duration. At the initial stage of contact, the skin and the object were assumed to be semi-infinite bodies in contact with no thermal resistance, and the interface temperature was solved with an analytical model. The remainder of the contact period included the effect of thermal flow and thermal resistance, and the interface temperature was solved using finite element methods.

Ho and Jones (2008) developed a thermal model based on a transient thermal process, where heat flux is transferred across the interface between the skin and object by conduction and flows through a thermal contact resistance. The skin and the object can both be modeled as semi-infinite bodies, if the contact time is short enough for the semi-infinite body model to be valid (Ho & Jones, 2006b). If this assumption is met, then the thermal model of the heat flux conducted out of the skin to the object can be described as follows:

$$q''(t) = k_{skin} A\left\{-e^{\alpha_{skin} B^2 t} erfc(B\sqrt{\alpha_{skin} t})\right\}$$

$$A = \frac{-(T_{skin,i} - T_{object,i})}{k_{skin} R} \qquad B = \frac{1}{k_{skin} R}\left[1 + \frac{(k\rho c)_{skin}^{1/2}}{(k\rho c)_{object}^{1/2}}\right]$$

where k is the thermal conductivity (W/m K), ρ is the density (kg/m^3), c is the specific heat ((J/kg K), α is the thermal diffusivity (m^2/s), t is the time (sec), R is the thermal contact resistance (m^2 K/W), and q" is the heat flux (W/m^2). The thermal contact resistance is based on the model proposed by Yovanovich (1981), which takes into account the mechanical, thermophysical, and surface properties with no fluid in the interfacial gap. The thermal contact resistance, R, is given by:

$$R = \left\{ 1.25 k_s \frac{\Delta a}{R_q} \left(\frac{P}{H} \right)^{0.95} \right\}^{-1}$$

where k_s is the harmonic mean thermal conductivity of the interface, R_q is the effective root-mean-square surface roughness, and Δa is the effective absolute average asperity slope, H is the microhardness of the softer material (which in this case is the skin), and P is the contact pressure. In this model, the heat flux exchanged during contact is a function of time, thermal contact resistance, and the initial temperatures and thermal properties of the skin and the object.

1.5 Objectives of Research

The objectives of the research conducted for this thesis were to understand the thermal response of the finger pad and how these responses influenced the perceptual changes that occur under different contact conditions. The thermal response of the finger pad was measured as the contact force changed from 0.1 to 6 N as well as a function of the surface texture in contact with the finger. The effect of varying surface texture on the perception of temperature was also investigated. In the final set of experiments the effect of varying the surface temperature of the thermal display on the perceived magnitude of the finger force was studied.

The thesis is organized in the following way. In Chapter 2, an experiment designed to understand the effect of contact pressure on the thermal response of the hand is described. In this study, an infrared thermal imaging system was used to measure key parameters including the contact area and temperature distribution on the finger pad during contact. Chapter 3 describes an experiment conducted to determine the effect of surface roughness on the thermal response of the finger pad. In Chapter 4, a psychophysical experiment is described that determined how surface roughness affects the perception of temperature changes on the finger.

In Chapter 5, a thermal display was developed using two Peltier devices to examine whether contact temperature influences the perception of applied force. One finger generated a target force on a thermal display whose surface temperature varied. The opposite finger simultaneously made contact with a thermal display whose surface temperature was maintained at 32 °C, and the subject was asked to match the force applied by two fingers. The goal of this experiment was to determine how the perception of force is affected by changes in temperature.

Chapter 6 provides a summary of the conclusions of this research as well as potential areas of future work.

2 Effect of Contact Pressure on Thermal Responses of the Hand

A change in skin temperature occurs when the finger generates a force against an object and the finger pad is compressed. Compression of the finger pad affects temperature in two ways: first, by increasing the contact area which allows for a higher heat flux (Greenspan & Kenshalo, 1985), and second, by restricting blood flow in the capillary network beneath the skin's surface which should contribute to a decrease in temperature of the finger pad (Mascaro & Asada, 2001). When the contact area between the finger pad and an object increases, there is a greater surface area for heat transfer. The relationship between contact area and force is dependent on the viscoelastic properties of the finger pad. Most of the change in contact area occurs at low forces before the load reaches 1 N when the finger pad is relatively compliant (Serina et al., 1997). The collapse of blood vessels at high contact forces may also affect the skin temperature as blood flow is driven away from the contact area into the capillaries under the nail bed. At low contact forces up to about 0.5 N, there is capillary perfusion of the finger pad. At higher contact forces, there is a progressive decrease in blood flow which is reduced by 70% at 3 N as compared to that occurring at 0.5 N (Jay & Havenith, 2006).

When an object is held in the hand, a transient thermal response occurs which is dependent on the contact conditions which influence the heat flux conducted out of the skin during contact. The aim of this experiment was to investigate how contact pressure affects the change in temperature of the finger pad. Contact pressure was computed as a function of the contact force and contact area of the finger pad. The contact forces

ranged from 0.1 to 6 N which are within the range of forces used in grasping tasks and manual exploration of objects (Shimoga, 1993; Sutter et al., 1989).

2.1 Method

Subjects. Ten normal healthy adults volunteered to participate in this study. There were seven males and three females ranging in age from 19 to 51 years old, with a mean of 27 years old. The subjects had no known abnormalities of the tactile, proprioceptive, or thermal sensory systems and no history of peripheral vascular disease. All subjects reported that they were right handed. This research was approved by the MIT Committee on the Use of Humans as Experimental Subjects.

Apparatus. An infrared based camera system shown in Figures 2-1 and 2-2 was used to measure the temperature of the right index finger pad as subjects made contact with a barium fluoride (BaF_2) window. The BaF_2 window (Crystan Ltd.) was 43 mm in diameter and 10 mm thick. The BaF_2 material was chosen because it is transparent to both infrared radiation and visible light. It also has a high contact coefficient and high stiffness as seen in Table 2.1.

Table 2.1. Properties of BaF_2 contact material

Material Property	**BaF_2**
Conductivity k [W/mK]	11.7
Density ρ [kg/m^3]	4890
Specific heat c [J/kgK]	410
Contact coefficient $(k\rho c)^{1/2}$ [$J/m^2s^{1/2}k$]	4843
Young's Modulus E [GPa]	53.1

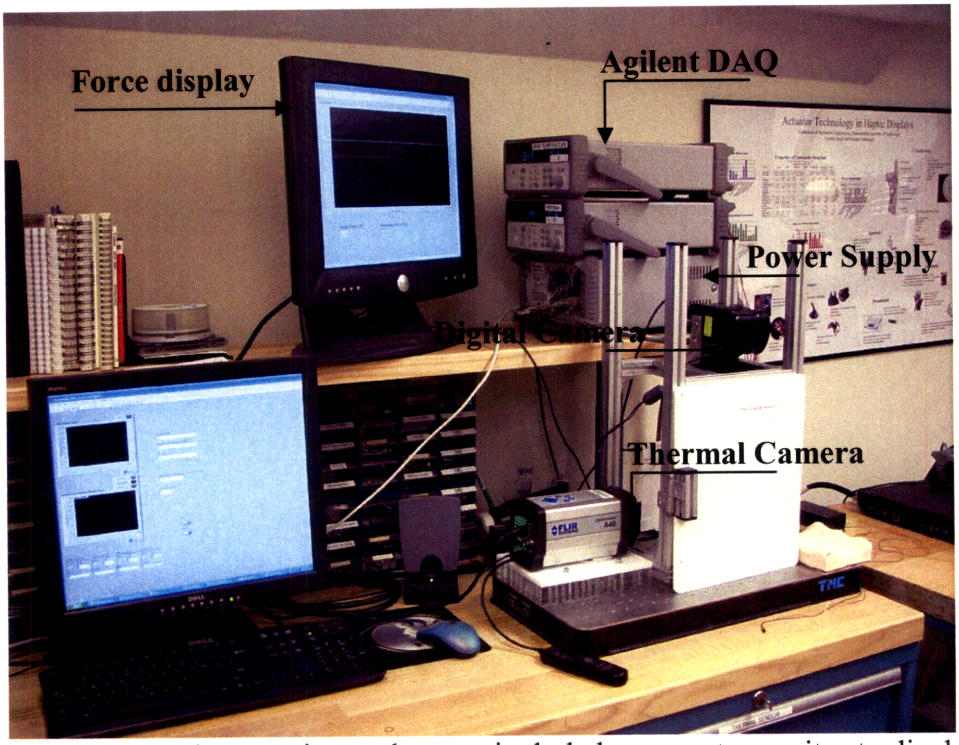

Figure 2-1. The experimental set-up included a separate monitor to display target and measured force values to the subject.

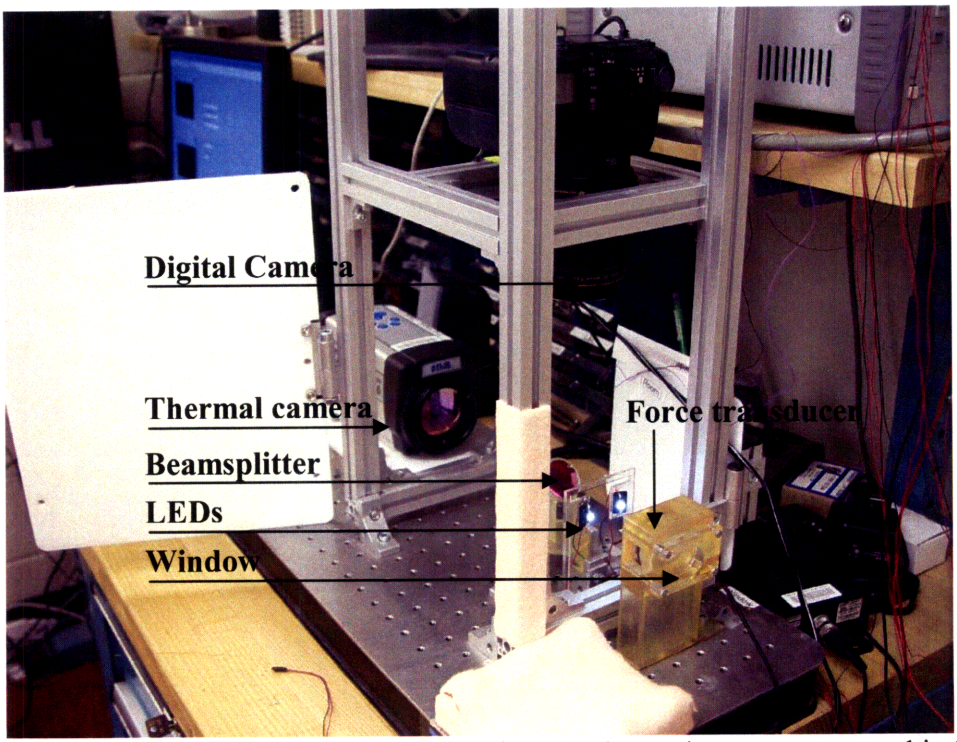

Figure 2-2. Experimental set-up showing the thermal camera mounted in line with the beamsplitter, and BaF_2 window. The 6-axis force transducer is located in the same fixture as the BaF_2 window, closer to the thermal camera. The LEDs are mounted in between the beamsplitter and the force transducer. The digital camera is mounted above.

The thermal camera (A40M, FLIR Systems) used to measure the temperature of the finger pad was connected to a computer via a Firewire cable, and controlled using a software package provided by the manufacturer (ThermaCam Researcher SR-3, FLIR Systems). The spatial resolution of the image recorded by the thermal camera was 400 μm, which is sufficient for capturing thermal information on the finger pad (Ho & Jones, 2006a).

As shown in Figure 2-2, a beamsplitter made of germanium (Ge) with anti-reflective coating, was used to separate the infrared radiation and visible light. The beamsplitter measured 32 mm in diameter and was 3 mm thick. A digital camera (EOS D60, Canon) with a 100 mm macro lens (EF 100 mm, Canon) was used to take images of the finger in contact with the window. It was controlled by a manual remote control, and images were stored on a CF card, which were moved onto the computer for processing after completion of all of the trials. Two LEDs (Luxeon III Emitter, LumiLEDs) were attached to a thin clear acrylic structure in between the beamsplitter and BaF_2 window to provide additional light to the finger pad for the digital image capture as seen in Figure 2-2. The LEDs were connected to a DC power supply (Model E3632A, Agilent Technologies).

A 6-axis force transducer (Nano 43, ATI Industrial Automation) with a 20 mm hole in the center was mounted next to the BaF_2 window, and measured the force exerted by the finger without obstructing the infrared and visible light (Ho & Jones, 2007, 2008). Force was sampled at a rate of 80 Hz by a data acquisition card (NI PCI-6023E, National Instruments) inside the computer. A separate monitor was used to graphically display the target and measured force values to the subject. The output of the force transducer was

processed by the data acquisition card, and sent to the monitor connected to the computer. The fixtures that held the force transducer and window, as well as the beamsplitter, were made with a rapid prototyping system (Viper Laser Stereolithography Forming Center, 3D Systems).

Four thermistors (457 μm diameter, 3.18 mm length; Model 56A1002-C8, Alpha Technics) with a sampling rate of 1 Hz were used to measure the temperature of the finger pad, BaF_2 window, beamsplitter, as well as the ambient temperature. The thermistors were connected to two data acquisition units (Model 34970A, Agilent Technologies), which were connected to the computer via a USB/GPIB interface (Model 82357A, Agilent Technologies) and controlled using the Labview 8.5 program as seen in Figure 2-1.

A recirculating chiller (Model 1167P, VWR International) was used to maintain the skin temperature at 33 °C at the start of the experiment, and between trials prior to making contact with the window. The recirculating chiller was connected to a spiral folded tube (4.8 mm ID, 7.9 mm OD) inside of a delrin fixture. A 2 mm thick copper plate was placed on top of the spiral folded tube to improve temperature uniformity of the surface. A 3.2 mm thick rubber pad was positioned on top of the copper plate for added comfort when subjects placed their hands on it to maintain skin temperature.

Procedure. Upon arrival, each subject's finger pad was cleansed with a cotton swab of isopropyl rubbing alcohol (70%) (CVS pharmacy). A thermistor was glued on the right index finger pad on the edge of the contact area using a biocompatible cyanoacrylate (Liquid Bandage, Johnson & Johnson). Medical tape (Nexcare) was used to secure the thermistor leads along the hand and wrist as shown in Figure 2-3. Subjects' initial skin

temperatures ranged from 29.3 to 35.6 °C, with an average value of 33.0 °C. The room temperature was maintained at approximately 23 °C, and measured with a thermistor in free air.

Subjects initially placed their right hands on the chiller pad to bring them to a preset temperature of 33 °C. A series of auditory cues generated in the Labview program paced the sequence of events. At the first sound cue, subjects removed their right hand from the chiller pad, and placed their right index finger in a holding position. At the second sound cue, subjects made contact with the contact surface and generated a force that matched the target force displayed on the monitor by pushing against the BaF_2 window with their finger. The monitor displayed the target force as a white line and the force the subject was generating as a red line. The two forces were also displayed on the screen below the graph as a digital readout. A third sound cue was heard after 10 or 20 seconds to indicate that the subject should remove their finger from the BaF_2 window and place it back on the chiller pad for at least one minute to maintain skin temperature. Labview recorded the skin, window, beamsplitter, and ambient temperature at a sampling frequency of 1 Hz, which was sufficient to capture the change in temperature. This sequence of events was repeated for each force value and contact duration.

Nine contact forces were produced (0.1, 0.25, 0.35, 0.5, 1.0, 1.5, 2, 4, 6 N), and there were two contact durations of 10 and 20 seconds. Two trials were performed for each 10-second contact duration, and one trial was performed for the 20-second contact duration. A thermal image and a digital camera image were manually taken when the subject first matched the required target force, and at the end of the contact period. The thermal camera was controlled using a manual trigger in the ThermaCam Researcher SR-

3 software program (FLIR Systems), and the digital camera image was taken with a manual remote.

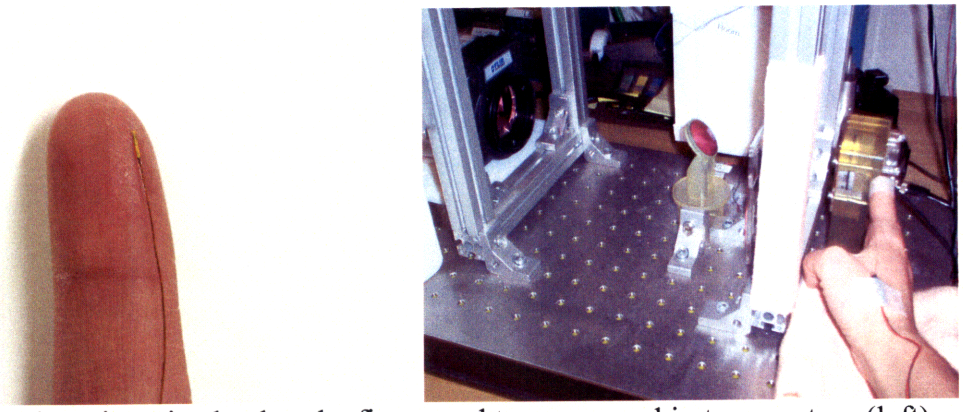

Figure 2-3. A thermistor is glued to the finger pad to measure skin temperature (left). Medical tape was used to secure the thermistor on the hand and along the wrist as the finger made contact with the BaF_2 window in the experimental apparatus (right).

2.2 Results

Thermal images were used to determine the change in contact area of the finger pad on the BaF_2 window as a function of force. The perimeter of the contact area was manually outlined on the thermal image in ThermaCam Researcher SR-3 software (FLIR Systems, Inc.). The images were converted to binary black and white scale in Adobe Photoshop CS (Adobe Systems, Inc.) and then processed in Matlab (MathWorks, Inc.) to determine the contact area. Figure 2-4 shows a characteristic set of thermal images from one subject.

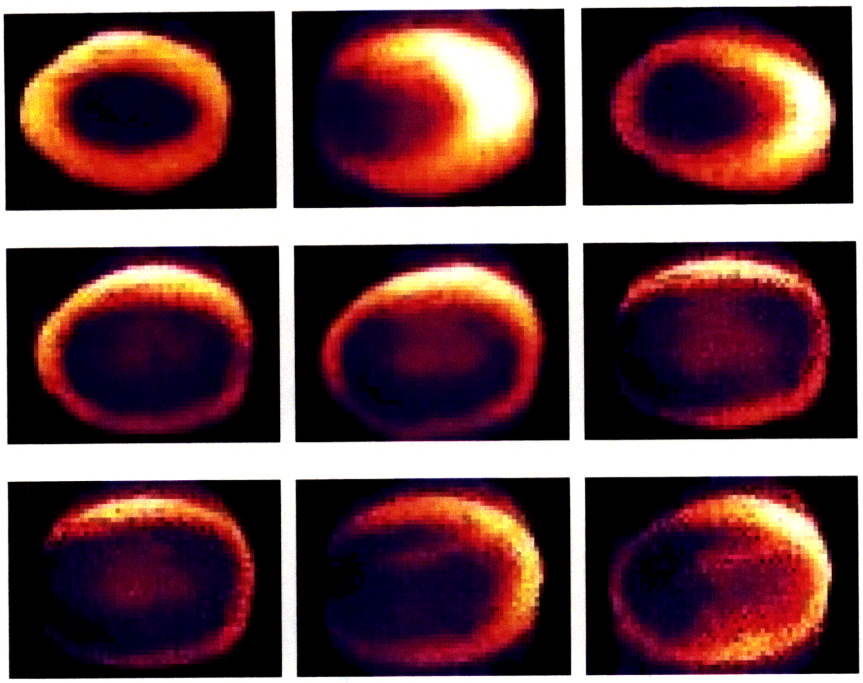

Figure 2-4. Thermal images for one subject across force levels ranging from 0.1 to 6.0 N. Left to right, first row: 0.1, 0.25, 0.35 N; second row: 0.5, 1.0, 1.5 N; third row: 2.0, 4.0, 6.0 N.

The relation between force and the mean contact area is shown in Figure 2-5. A logarithmic function fitted to the data accounted for 90% of the variance. As can be seen in the figure, there is a rapid increase in contact area at low forces with a 86 mm^2 increase in contact area between 0.1 and 2 N. Over 70% of this change occur at contact forces below 1 N.

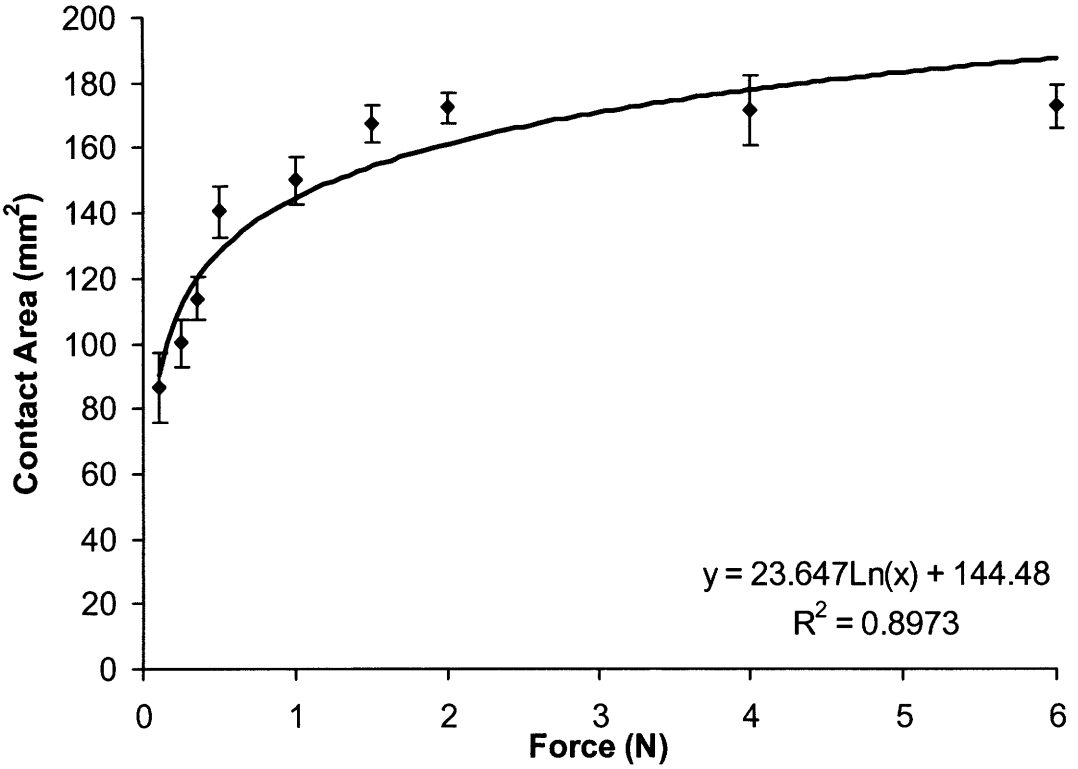

Figure 2-5. Relation between contact force and mean contact area averaged across 10 participants. The error bars represent the standard error of the mean. The logarithmic function fitted to the data is also shown.

The thermal images in Figure 2-4 visually depict what the graph in Figure 2-5 shows, namely that the contact area increases rapidly at low force levels, and appears to reach a maximum value at around 2 N when the finger pad is fully compressed.

The change in skin temperature during contact was computed as the difference between the initial skin temperature as measured by a thermistor on the finger pad and the average temperature across the finger pad calculated from the thermal image taken at the end of the contact period. The temperature of the finger pad on the thermal image was evaluated based on the total energy detected (U_{tot}) by the thermal camera. The uncalibrated object signal is a measure of the total energy detected, including radiation from the atmosphere and external optics, such as the Ge beamsplitter and BaF_2 window.

Based on radiosity concepts, it is possible to determine the target temperature of the finger pad as a function of the energy received by the camera using the thermal camera calibration curve. Equation (1) shows the contribution of the emissivity, transmissivity, and reflectivity of the window, beamsplitter, and ambient conditions:

$$U_{tot} = \varepsilon_{obj}\tau_1\tau_2 U_{obj} + (1-\varepsilon_{obj})\tau_1\tau_2 U_{amb} + \varepsilon_2 U_2 + \varepsilon_1\tau_2 U_1 + \rho_2\tau_2 U_{amb} + \rho_2 U_{amb} \qquad (1)$$

where ε is the emissivity, τ is the transmissivity, ρ is the reflectivity, and U is the energy. Subscripts denote total (tot), object (obj), ambient (amb), contact material (1), and beamsplitter (2).

The energy is related to the temperature based on the thermal camera calibration curve, which has unique R, B, F values for each individual camera. The relationship is shown in Equation (2):

$$U_{obj} = \frac{R}{e^{B/T_{obj}} - F} \qquad (2)$$

where U_{obj} and T_{obj} represent the energy and temperature of the finger pad, respectively.

The mean decrease in skin temperature as a function of contact force is shown in Figure 2-6 for a contact duration of 10 seconds. The decrease in temperature was greatest at forces of 0.25 and 0.35 N and 4.0 and 6.0 N, and was smaller for forces between 0.5 and 4.0 N. The decrease in temperature averaged 5.5 °C across the nine force values.

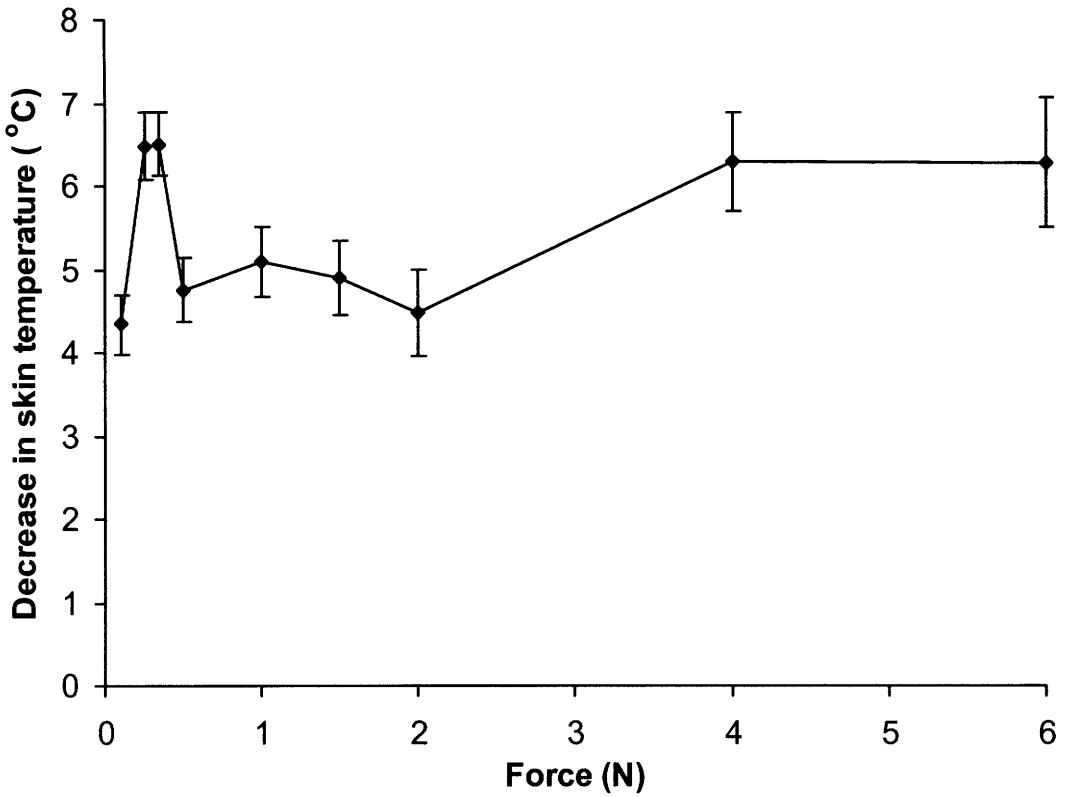

Figure 2-6. The decrease in skin temperature as a function of force after 10 seconds of contact averaged across 10 participants. The error bars represent the standard error of the mean.

A repeated-measures ANOVA with contact force as the within factor and change in temperature as the dependent variable indicated that there was a significant difference in temperature as a function of force, $F(3, 27) = 3.808$, $p = 0.021$ with Huynh-Feldt corrected df. The decrease in skin temperature was highly dependent on the magnitude of the contact force.

The change in skin temperature was also measured by the thermistor attached on the perimeter of the contact area, which was sampled at 1 Hz. The plot in Figure 2-7 shows the time course of the temperature data for each force level, averaged across ten subjects. The mean change in temperature recorded by the thermistor is seen in Figure 2-8.

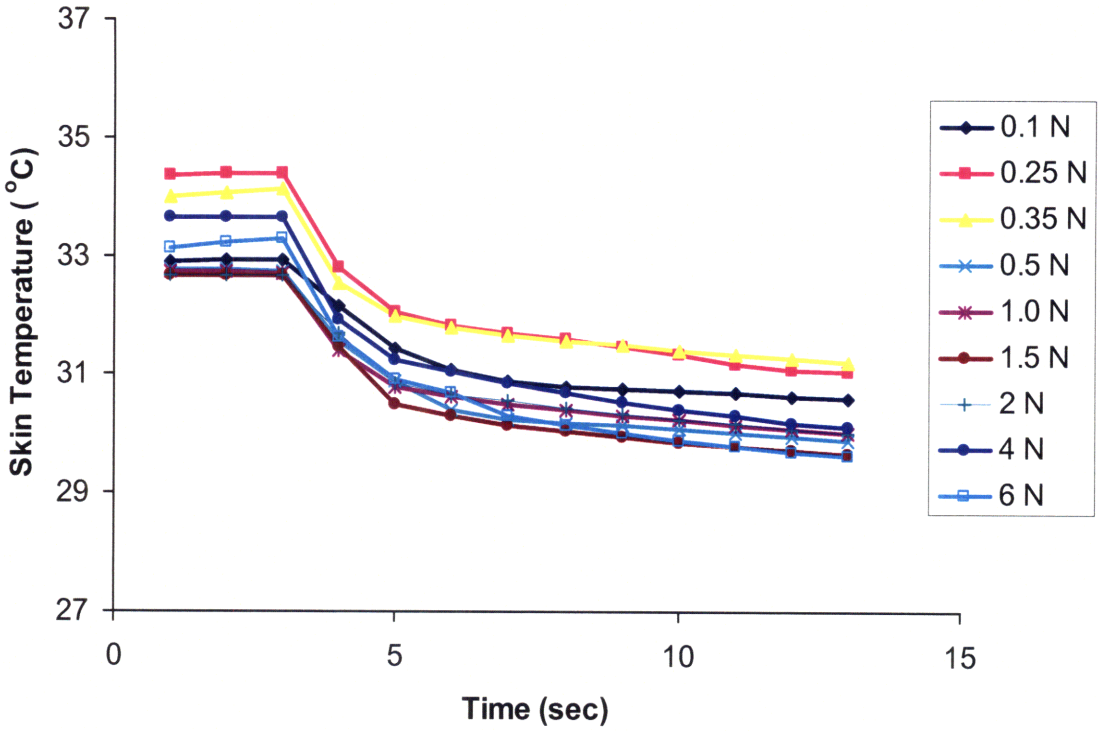

Figure 2-7. Time course of skin temperature change measured from a thermistor averaged across 10 subjects for each contact force.

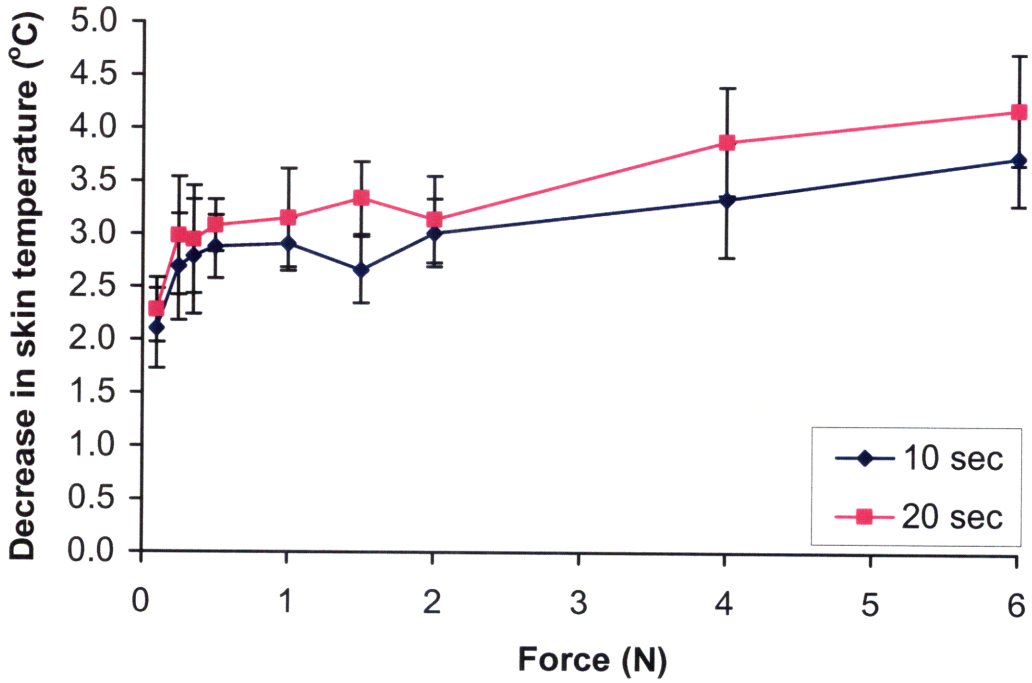

Figure 2-8. The decrease in skin temperature (based on thermistor data) as a function of contact force for 10 and 20 second contact periods averaged across 10 subjects. The error bars represent the standard error of the mean.

A repeated-measures ANOVA of the thermistor data with contact force and contact time as the within factors and change in temperature as the dependent variable indicated that there was a significant difference in the change of temperature as a function of contact force ($F(5, 43)= 2.592$, $p= 0.041$) and contact time ($F(1, 9)= 5.155$, $p= 0.049$) with Huynh-Feldt corrected df. The decrease in skin temperature was highly dependent on the magnitude of the applied contact force and the duration of the contact time.

The thermistor data in Figure 2-8 show a similar trend to the thermal image data in Figure 2-6, but with a lower overall average change in temperature of 3.1 °C across the range of forces. This indicates that the thermistor was not able to detect the full extent of the change in temperature even though it was located on the perimeter of the contact area. The temperature gradient from the center of contact outward to the perimeter of the contact area is captured in Figure 2-9. The temperatures are plotted along the line drawn across the contact area of the finger pad in the proximal to distal direction. The thermal image illustrates the localized nature of the change in skin temperature across the contact area.

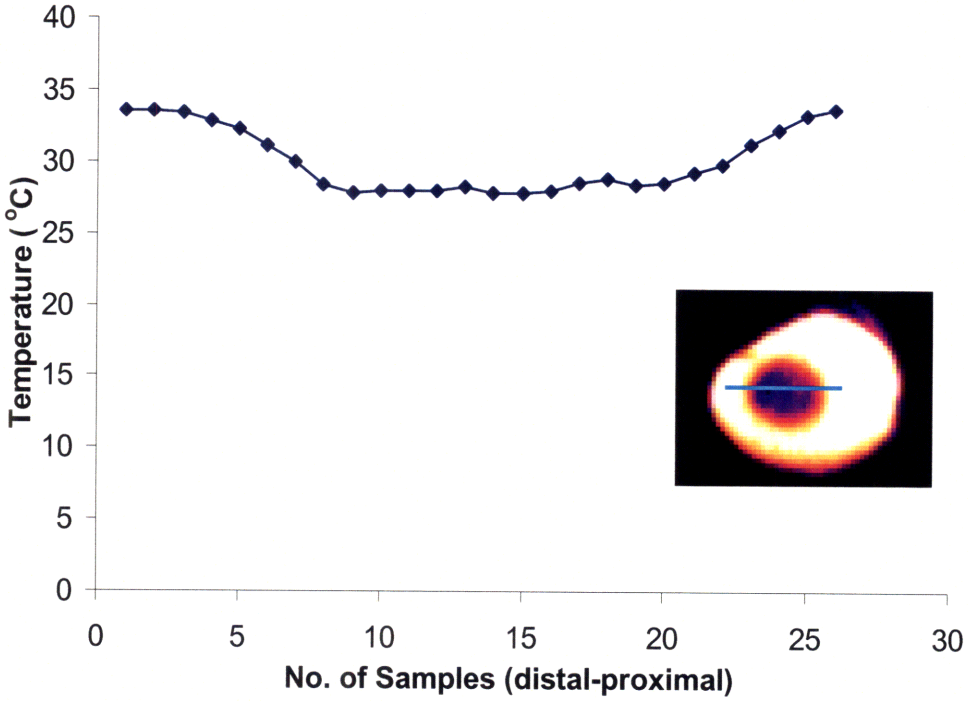

Figure 2-9. A plot of the temperature gradient across the contact area on the finger pad after 10 s of contact at a force of 0.1 N.

The contact pressure was calculated from the individual contact areas at each contact force, and averaged across all 10 participants. Figures 2-10 and 2-11 show the relationship between the decrease in skin temperature and contact pressure for thermal image and thermistor data, respectively.

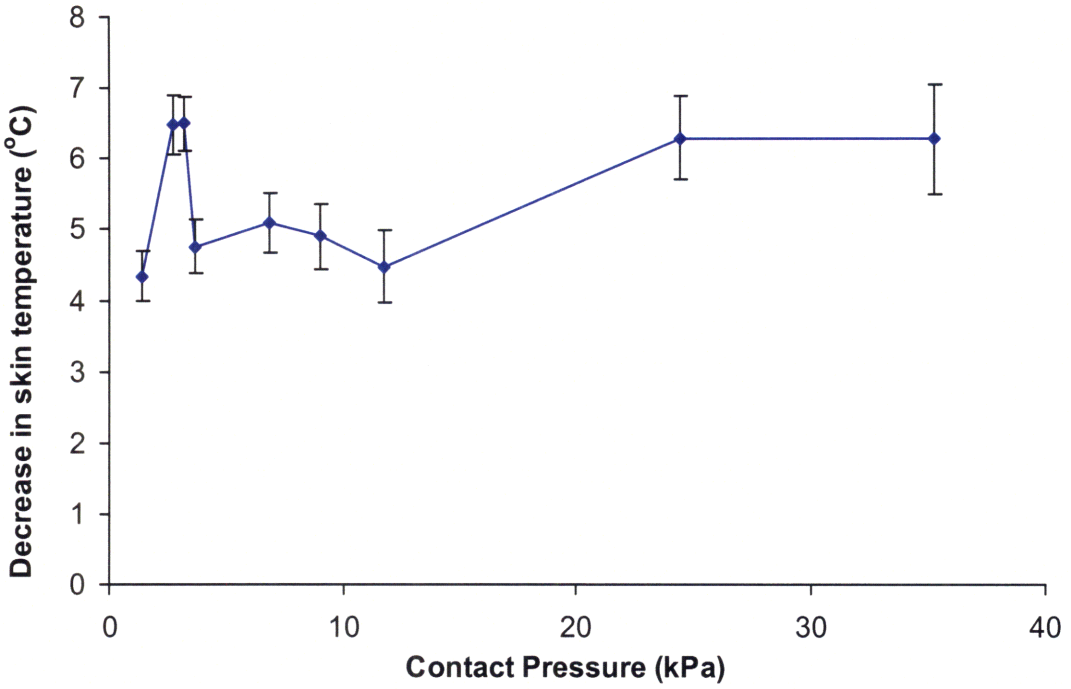

Figure 2-10. Decrease in skin temperature (measured from thermal images) as a function of contact pressure for 10 subjects after 10 seconds of contact. The error bars represent the standard errors of the mean.

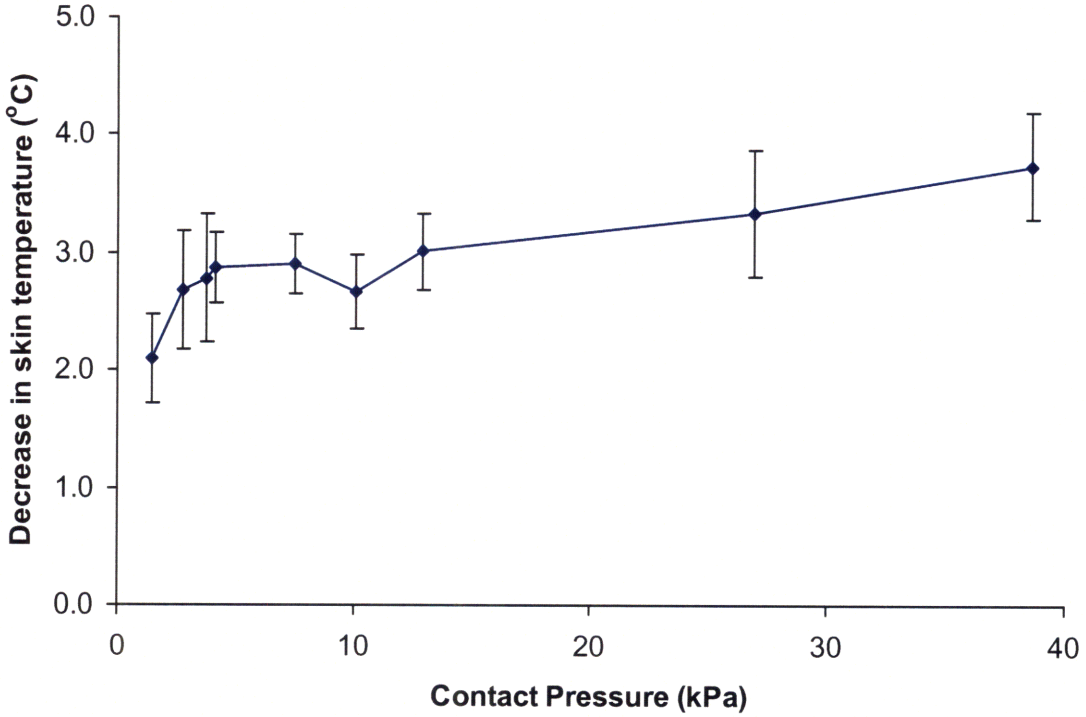

Figure 2-11. Decrease in skin temperature (measured from a thermistor) as a function of contact pressure for 10 subjects after 10 seconds of contact. The error bars represent the standard errors of the mean.

The contact pressure was calculated by dividing the contact force by the contact area of each subject's finger pad. As expected, the decreases in skin temperature as a function of contact pressure shown in Figures 2-10 and 2-11 are similar to the changes in temperature as a function of contact force. In Figure 2-10, the contact pressures for the corresponding nine forces were 1.41, 2.71, 3.19, 3.68, 6.82, 9.05, 11.71, 24.45, and 35.29 kPa. The greatest changes in temperature occurred between 2.71- 3.19 kPa and 24.45-35.29 kPa. The greater decreases in temperature found in the thermal image data in the 2.71- 3.19 kPa range were not present in the thermistor data presumably because of the thermistor's limitations in detecting the full extent of temperature decrease across the contact area. A comparison of the mean decrease in skin temperature as measured by the thermal camera and the thermistor after 10 s of contact across the 10 participants is shown in Figure 2-12.

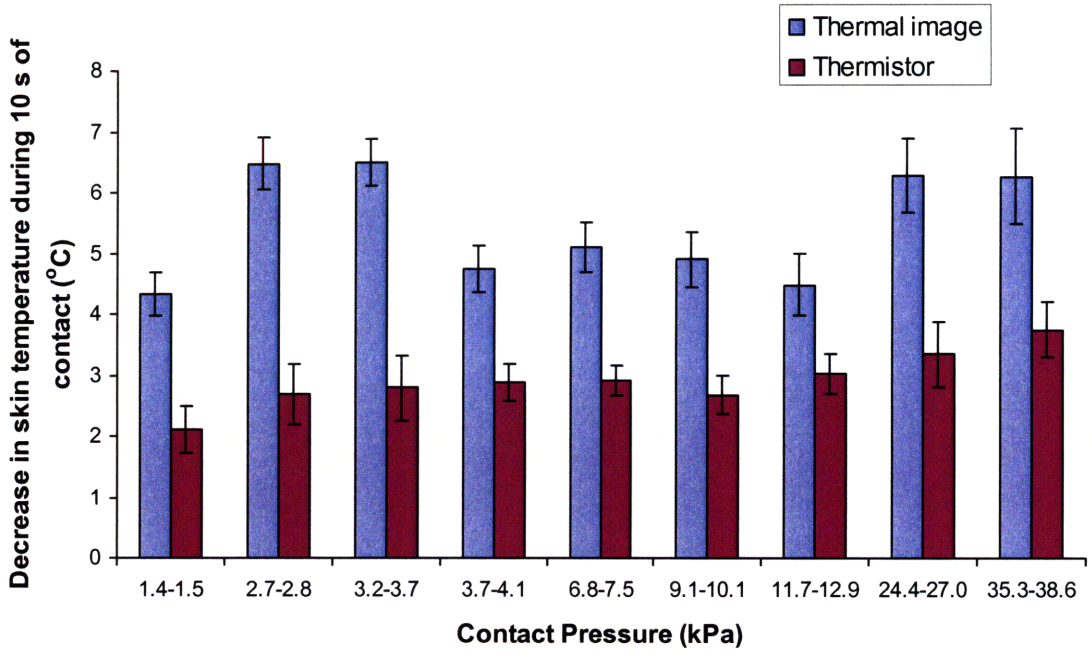

Figure 2-12. The mean decrease in skin temperature based on thermal image and thermistor data. The error bars represent standard errors of the mean.

2.3 Discussion

A number of thermal models have been developed to predict the change in skin temperature during contact with an object with the goal of incorporating thermal feedback into haptic devices. Most of these models are based on the bioheat equation formulated by Pennes (1948) each with different assumptions and boundary conditions. Current models have considered the effects of blood perfusion and the thermal and mechanical properties of the skin and contact material (Bergamasco et al., 1997; Citerin et al., 2006; Deml et al., 2006; Ho & Jones 2006a; Yamamoto et al., 2004; Yang et al. 2008). Ho and Jones (2006a) account for the thermal and mechanical properties of the skin and contact material, in addition to other factors such as contact pressure and thermal contact resistance.

The thermal model proposed by Ho and Jones (2006a) predicted that skin temperature would decrease as a function of contact pressure. A comparison between the theoretical predictions and the decreases in skin temperature measured using the thermal camera is shown in Figure 2-13. At contact pressures above 12 kPa, the model is very accurate, but at lower contact pressures it tends to underestimate the decrease in temperature. As seen in Figure 2-13, for contact pressures greater than 12 kPa (corresponding to a force of 2 N), the model predicts the measured temperature values to within 0.25 °C. For contact pressures less than 12 kPa, the theoretical prediction follows the general trend of the temperature data, but underestimates the decrease in temperature by an average of 2.7 °C. Ho and Jones (2008) examined contact pressures ranging from 0.73 to 10.98 kPa, which corresponds to a range of contact forces from 0.1 to 2 N. Their results are similar in that the model underestimated the decrease in temperature at contact

pressures below 3.14 kPa. For contact pressures larger than 5.90 kPa, the difference between the model and measured data was within 1 °C (Ho & Jones, 2008).

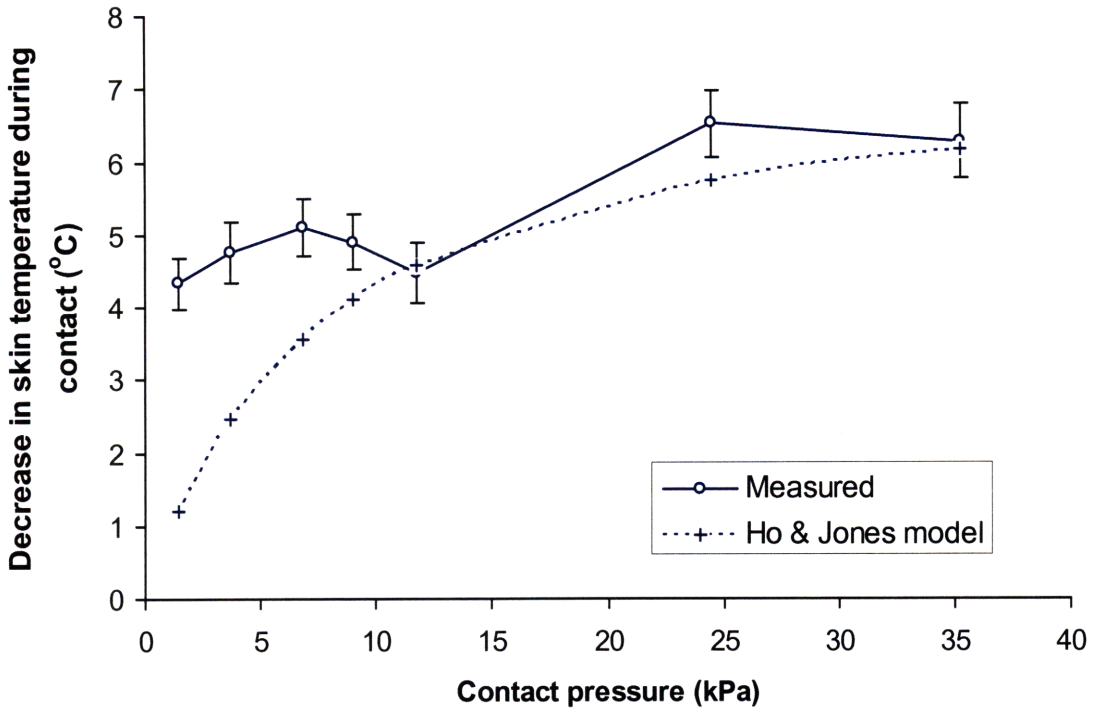

Figure 2-13. Measured and predicted changes in temperature based on the Ho and Jones thermal model (2006a). The error bars represent standard errors of the mean.

One possible explanation for the difference between the theoretical predictions and the experimental results may be the estimation of thermal contact resistance at low contact pressures. Thermal contact resistance is estimated based on the model proposed by Yovanovich (1981), which assumes that no fluid is present in the interfacial gap, and the resistance is a function of mechanical, thermal, and surface properties of the objects in contact. The Yovanovich model accounts for the effective root-mean-square surface roughness and absolute average asperity slope of the contact materials. Ho and Jones (2006a) measured these values for the fingerpad and the BaF_2 contact material, and implemented those values in their model. The Yovanovich (1981) model also includes

the microhardness of the softer material, which in this case is the skin. The microhardness value used in the Ho and Jones model (2006a) was 0.1225 MPa as reported by Dellon et al. (1995). The discrepancy between the predicted and measured results suggests that the model used for the estimation of thermal contact resistance may not be relevant for the range of contact pressures assessed in this experiment (1.41-35.29 kPa). The Yovanovich model (1981) is based on contact between two rigid bodies, where the ratio of contact pressure to microhardness is 1E-6 to 2E-2. In this study, the contact is between a rigid body and a soft tissue, where the ratio of contact pressure to microhardness of the skin was in the range of 0.01 to 0.3.

The thermal image data also indicated that there was a large decrease in skin temperature at low contact forces between 0.25 N and 0.35 N, which was not expected, and was not captured in the thermistor data. The vascular anatomy of the fingertip may provide insight into a plausible explanation for these results. The nail bed is richly vascularized with blood flowing from the digital arteries into the arterioles through a capillary network and back out through the venules and into the digital veins. The arteries that feed the nail bed are located above the bone, which is connected to the fingernail via collagen fibers. Consequently, the arteries above the bone are protected during contact at low forces, while the veins that drain the nail bed are located below the bone, closer to the palmar surface. The veins are also generally larger and more compliant than arteries, which make them more susceptible to collapse under pressure. As pressure is applied to the fingertip, the veins collapse and cause blood to pool in capillaries beneath the nail (Smith et al., 1991). The decrease in temperature of the finger pad would be expected to increase when the blood flow is constricted in this way.

There are two distinct zones of capillaries in the fingertip: the proximal reddening zone capillaries which are protected by the bone and nail structure, and the distal whitening zone capillaries that are susceptible to collapse by applied pressure. The nail bed capillaries at the distal end of the fingertip are not protected by the bone. As the pressure increases, these capillaries collapse and have a whitening effect on the finger nail (Mascaro & Asada, 2000). The resulting thermal effect would be a greater decrease in skin temperature during contact.

Thermal images indicated that at low forces, subjects tended to press against the contact material with the distal portion of their fingertip, as seen in the characteristic set of images in Figure 2-4. The greater decrease in skin temperature at these lower forces suggests the capillary network may have collapsed in the distal palmar surface of the fingertip. This would explain the greater decrease in temperature at the 0.25-0.35 N contact force, and at high contact forces between 4-6 N, where capillary perfusion is not present at all in the proximal or distal regions. In addition, the thermistor located on the perimeter of the contact area would not have been able to detect the localized change in temperature due to the collapse of capillaries on the contact surface.

The decrease in skin temperature stabilized within 2 seconds of contact with a temperature range of 4.3-6.5 °C for contact pressures up to 35 kPa. These results, shown in Figure 2-7, are comparable to results reported by Ino et al. (1993) and Yamamoto et al. (2004), who also showed a rapid decrease in skin temperature during the first 2 seconds immediately following contact, followed by a much slower decrease in temperature.

2.4 Conclusion

The results of this experiment indicate that contact pressure and contact duration have a significant effect on changes in skin temperature. The thermal response of the finger pad was evaluated over a comprehensive range of contact forces from 0.1 to 6 N. Current thermal models were unable to accurately predict the thermal response across the entire range of contact pressures, but gave accurate results for higher contact pressures. The infrared thermal measurement system was able to detect the temperature gradient across the finger pad during contact, and confirmed the localized nature of the thermal responses of the skin during contact. The thermistor data confirmed the general trend of data recorded by the infrared camera, and demonstrated the limitations of point contact sensors.

3 Effect of Surface Roughness on Thermal Response of the Hand

The purpose of this experiment was to examine how the surface roughness of an object influences the heat flux conducted out of the skin during contact. Several studies have investigated the effect of surface roughness on tactile sensation, but the thermal response has rarely been evaluated. Simulations based on the Ho and Jones (2008) thermal model indicate that skin temperature will change as a function of surface roughness, and that the decrease in skin temperature will be greater when the hand is in contact with a smoother surface. Quantitative studies of the sensory perception of roughness use surfaces such as sandpaper, metal gratings, and fabrics that have features with a defined spatial period. Smooth surfaces are defined as having smaller spatial periods, and rough surfaces have larger spatial periods. Neurophysiological experiments routinely use plastic surfaces with embossed, tetragonal dot patterns, in which each dot has the shape of a truncated cone (Connor et al., 1990). The spatial periods that have been investigated in embossed plastic stimuli range from 0.8 to 6.5 mm (Connor et al., 1990). Rectilinear arrays of truncated pyramids have also been used as test stimuli (Hollins et al., 2001). Truncated pyramid patterns are produced by photolithography and wet chemical etching on silicon wafers, and achieve spatial periods ranging from 0.16 to 3.2 mm (Hollins et al., 2001).

The test stimuli used in this set of experiments consist of a rectilinear array of truncated pyramids, similar to the spatial patterns used by Hollins et al. (2001). However, the material and method of machining are different. Copper was chosen as the surface material because of its high contact coefficient and thermal conductivity, low

deformation, resistance to moisture from the finger pad, and machinability. A process using wire electrical discharge machining (EDM) was used to create the desired geometry. The range of spatial periods that was machined was limited by the spark gap and wire diameter of the EDM system. The spatial periods of the copper surfaces range from 0.8 to 3.0 mm. The thermal response of the finger pad was evaluated upon contact with six stimuli of varying spatial period.

3.1 Method

Subjects. Ten normal healthy adults volunteered to participate in this study. There were six males and four females ranging in age from 20 to 51 years old, with a mean age of 30 years old. Six of the ten subjects participated in the previous experiment involving contact pressure. The subjects had no known abnormalities of the tactile, proprioceptive, or thermal sensory systems and no history of peripheral vascular disease. The subjects reported that they were right handed. This research was approved by the MIT Committee on the Use of Humans as Experimental Subjects.

Apparatus. The surfaces of six copper blocks (25.5 x 28.5 mm, 6 mm thick) were machined with a pattern of truncated pyramids using a wire EDM method (Charmilles Technologies Robofil 1020SI Wire EDM) as seen in Figures 3-1 and 3-2. The truncated pyramids had a constant height of 0.5 mm, and were spaced at periods of 0.80, 1.0, 1.5, 2.0, 2.5, and 3.0 mm to produce a range of surface textures. The material properties of copper are shown in Table 3.1.

Table 3.1. Material properties of Copper

Material Property	Copper
Conductivity k [W/mK]	398
Density ρ [kg/m^3]	8954
Specific heat c [J/kgK]	384
Contact coefficient $(k\rho c)^{1/2}$ [J/m^{2}s$^{1/2}$k]	36992
Young's Modulus E [GPa]	110.0

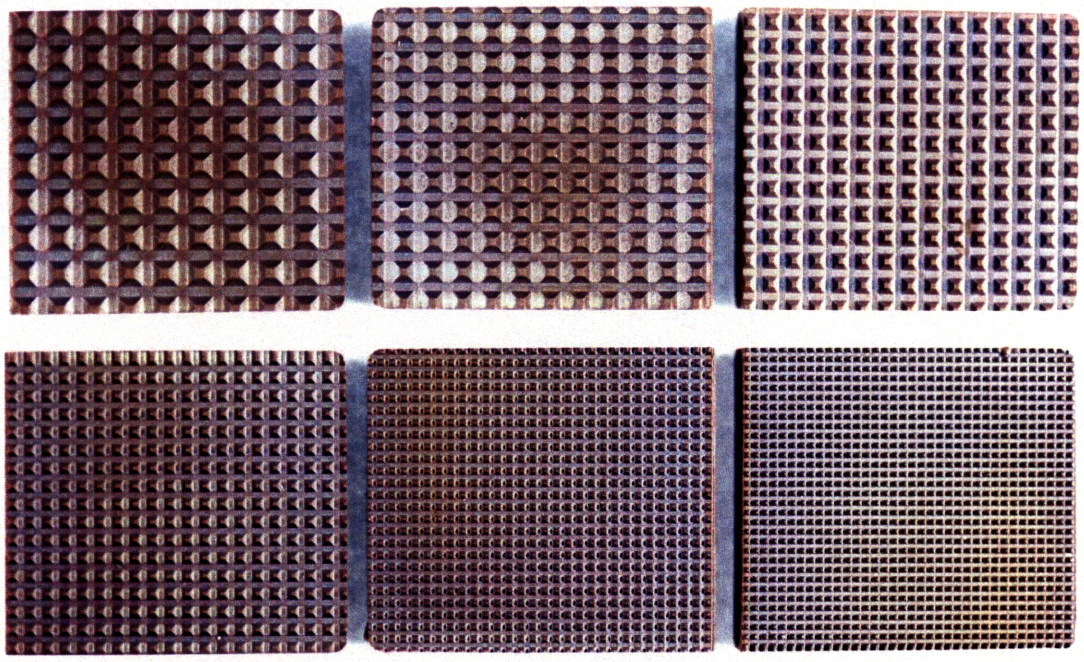

Figure 3-1. Copper test stimuli with truncated pyramids (top row, left to right: spatial periods of 3.0, 2.5, 2.0 mm; bottom row, left to right: spatial periods of 1.5, 1.0, 0.80 mm). The height of the pyramids for each spatial period is 0.5 mm.

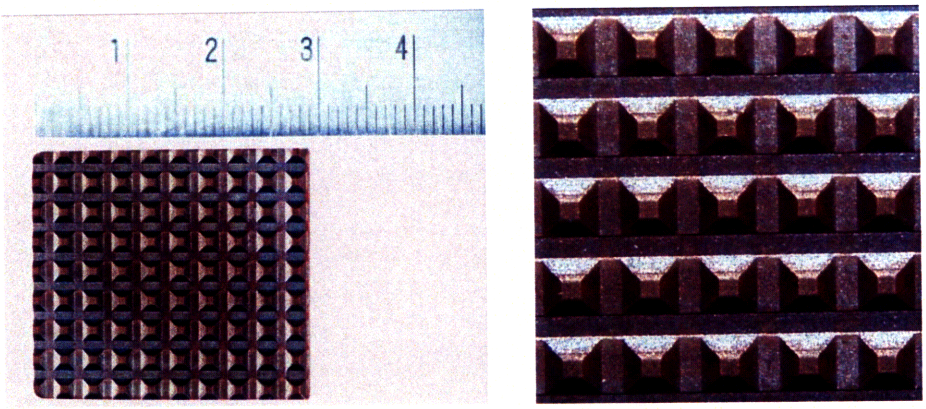

Figure 3-2. One copper test stimulus with spatial period of 2.5 mm and height of 0.5 mm.

A thermistor (457 μm diameter, 3.18 mm length; Model 56A1002-C8, Alpha Technics) was glued to the edge of the contact area of the right index finger pad with a biocompatible cyanoacrylate (Liquid Bandage, Johnson & Johnson). Another thermistor was mounted in free air to record the ambient temperature of the room, which was maintained at approximately 23 °C. Both thermistors were connected to a data acquisition unit (Model 34970A, Agilent Technologies), which was controlled with a Labview 8.5 program. A digital force gauge (Model DFS-20, SHIMPO) was mounted on a fixture at elbow height to allow subjects to comfortably press down on each copper block with their right index fingers as seen in Figure 3-3. The force gauge was connected to a shielded connector block for analog I/O (Model NI BNC-2110, National Instruments) that was in turn connected to a data acquisition unit (NI DAQCard-6036E, National Instruments) in the computer. An aluminum fixture was constructed to hold the copper block in place on the digital force gauge. The force gauge was zeroed when the weight of the aluminum fixture and the copper block were placed on it.

The force gauge was calibrated with a set of calibrated weights. The voltage output was measured in the experimental set-up with the Labview 8.5 program. The

following calibrated weights were placed on the force gauge: 10 g, 20 g, 50 g, 100 g, 200 g, 500 g. The relationship between the voltage measured and the force applied was linear with a R^2 value of 0.9999.

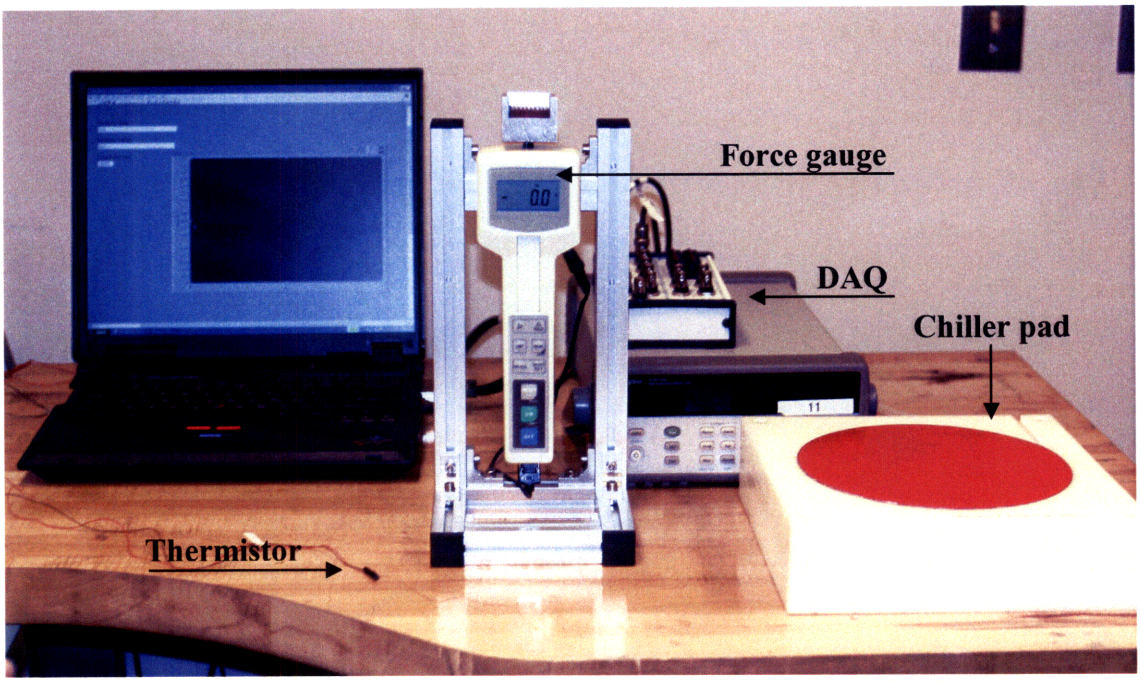

Figure 3-3. Experimental set-up for measuring the temperature change as a function of spatial period. The recirculating chiller pad is shown to the right of the force gauge.

Procedure. Upon arrival, each subject's finger pad was cleansed with a cotton swab of isopropyl rubbing alcohol (70%) (CVS pharmacy). A thermistor was glued using a biocompatible cyanoacrylate (Liquid Bandage, Johnson & Johnson) on the right index finger pad so as not to interfere with contact. Medical tape (Nexcare) was used to secure the thermistor leads along the hand and wrist. Subjects' initial skin temperatures ranged from 29.5 to 36.1 °C, with an average value of 32.1 °C. The room temperature was maintained at 23 °C, and measured with a thermistor in free air.

All of the copper test stimuli were stored at room temperature. Each of the six blocks was presented three times for a total of 18 trials per subject. The order of

presentation of each copper block was randomized. There was at least a one minute break between trials, during which subjects placed their right hand back on the recirculating chiller to maintain the skin temperature at 33 °C.

Subjects were presented with three auditory cues generated by the Labview program, which indicated the sequence of the experiment. Subjects began with their right hand on the chiller pad. At the first sound cue, subjects removed their hand from the chiller pad and placed it in a holding position. At the second sound cue, subjects were instructed to make contact with the copper surface for 10 seconds at a constant force of 1 N. The third sound cue signaled the end of the 10-second contact interval and subjects removed their finger from the block and replaced it back onto the chiller pad. Labview recorded the skin temperature and ambient data at a sampling frequency of 1 Hz, which was sufficient to capture the change in temperature. It was not possible to capture the change in temperature of the surface of the copper block in this experiment. Several methods were tried, including embedding a thermistor below the contact surface, and taking a thermal image directly after contact. The copper block did not hold a thermal signature that could be captured after 10 seconds of contact with the finger.

3.2 Results

The spatial period is used to define the surface roughness of the copper surface, where smooth and rough surfaces are characterized by small and large spatial periods, respectively. For the test stimuli in this experiment, the spatial period is equal to $4a$, where a is the dimension shown in Figure 3-4. The height of the truncated pyramids for all spatial periods is 0.5 mm.

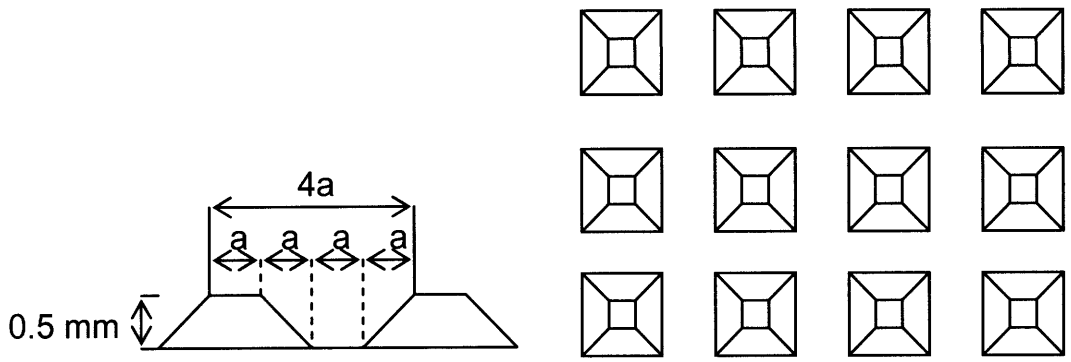

Figure 3-4. Geometry of the truncated pyramids on the copper surfaces.

A surface profilometer (SurfTest SV-3000S4, Mitutoyo) was used to measure the height and spatial period of the six test stimuli. The positional accuracy is 0.05 μm in the x-axis in the plane of the 4*a* spatial period, and 1 μm in the z-axis in the plane of the height of the truncated pyramids. The stylus tip shape is a 60 degree cone with a tip radius of 2 μm. The measured average height of the pyramids was 0.44 mm. The difference between the measured and the programmed height of the pyramids may have been due to the manual positioning of the truncated pyramids under the stylus tip. Especially for smaller spatial periods, it was difficult to visually align the tops of the pyramids under the measurement stylus. However, the spatial period measurements were very accurate for the six surfaces, as shown in Table 3.2.

Table 3.2. Measured spatial period of six test stimuli

Nominal Period (mm)	Measured Period (mm)	Difference
3.0	3.034	0.034
2.5	2.498	-0.002
2.0	2.021	0.021
1.5	1.501	0.001
1.0	1.004	0.004
0.8	0.800	0.000

The temperature of the finger pad, as measured by a thermistor, was recorded during contact with each copper test stimulus. The decrease in skin temperature as a function of the spatial period of the copper surface was relatively small as shown in Figure 3-5.

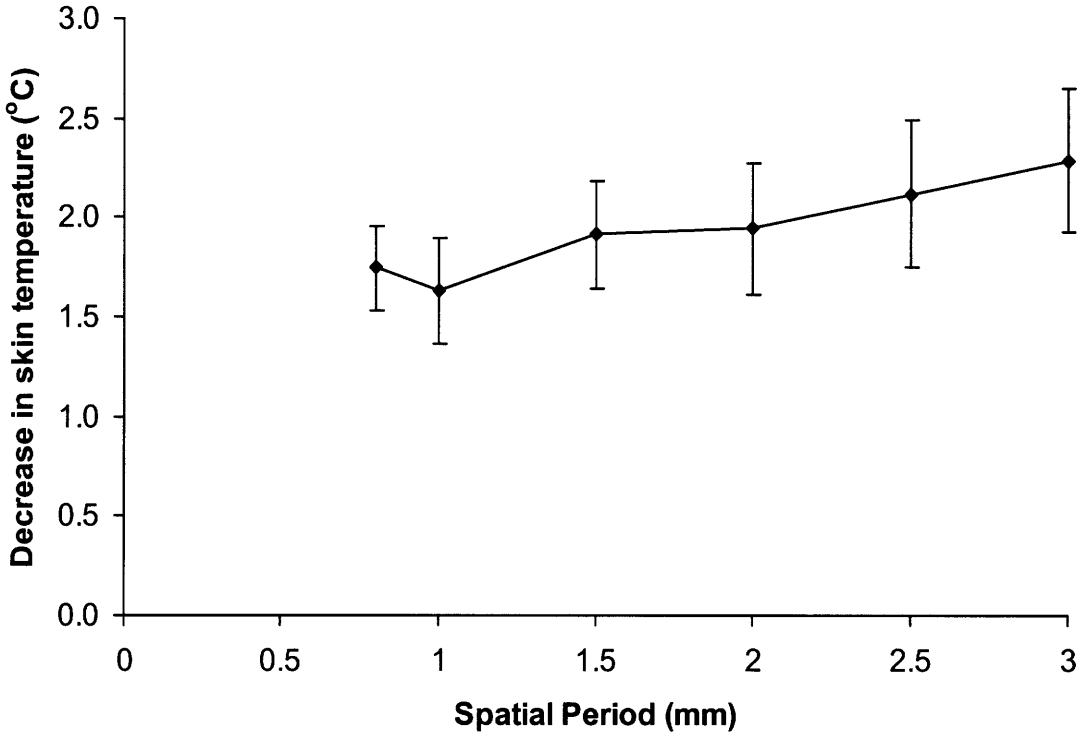

Figure 3-5. Decrease in skin temperature as a function of spatial period of the copper surface averaged across 10 participants. The error bars represent the standard error of the mean.

The data in Figure 3-5 show that as the surface became rougher, there was a progressive decrease in temperature during contact. The overall change in temperature was 0.54 °C between 0.8 mm and 3.0 mm spatial periods, whereas the mean decrease in skin temperature averaged across the six spatial periods was 1.94 °C. A repeated-measures ANOVA with the spatial period as the within subjects factor, and the change in temperature as the dependent variable indicated that there was not a significant difference

in the change in temperature as a function of the spatial period of the stimulus ($F(2, 21)= 2.099$, $p= 0.141$). However, there was a significant linear trend ($p=0.026$), which suggests that there is a small but consistent decrease in skin temperature as a function of spatial period. These results will be used to evaluate how surface roughness influences the perception of temperature during contact.

3.3 Discussion

The range of spatial periods chosen for this experiment is comparable to those used in other studies examining the perception of surface roughness (Connor et al., 1990; Dépeault et al., 2008; Hollins et al., 2001; Meftah et al., 2000). These studies focus on the effect of surface roughness on tactile sensation, and have not examined the effect of roughness on the thermal responses of the skin. It has been shown that cooling the skin affects the perception of roughness (Green et al., 1979), but there are no data that indicate how the temperature of the skin changes with surface roughness.

Ho and Jones (2006a) performed simulations of the effect of surface roughness on the heat flux conducted out of the skin when in contact with a copper surface. The thermal model used defined surface roughness in terms of the root-mean-square (RMS) surface roughness and asperity slope. The contact pressure and microhardness of the skin were also included in the model. Simulations were performed for RMS values equal to 8 and 30 μm, which are typical surface roughness values obtained from milling and sawing processes, respectively (Kalpakjian, 1995). The simulations indicated that surface roughness can influence the heat flux conducted out of the skin within 1 second of initial contact, and also that a larger decrease in skin temperature would occur when the hand was in contact with a smoother surface.

The results in Figure 3-5 suggest that the opposite is true, that is, there is a greater decrease in temperature when the hand is in contact with a rougher surface. The disparity between the results and the simulation may be due to the model used to estimate thermal contact resistance. The model predicted that the thermal contact resistance for the 0.8 mm copper stimulus was equal to 0.005 m^2K/W, and the thermal contact resistance of the 3 mm copper stimulus was equal to 0.010 m^2K/W. The model predicted that the smoother surface would have the lower thermal contact resistance, and therefore there would be a greater heat flux out of the skin during contact and a greater decrease in skin temperature. The thermal contact resistance model of Ho and Jones (2006a) was based on those of Benali-Khoudaja et al. (2003) and Yovanovich (1981). As noted in the previous experiment, the Yovanovich model is based on two rigid bodies in contact, which is not the case in this experiment, where soft tissue is in contact with a rigid copper surface.

The interface formed between contacting surfaces can play a major role in the thermal network that is established (Fedasyuk, 2003). It may be necessary to incorporate the geometric properties of the surfaces in contact, in addition to the RMS surface roughness and the asperity slope. The geometry and spatial period of the copper test stimuli in this experiment may have affected the contact area of the skin with the surface. For larger spatial profiles, the truncated pyramids are separated by a larger distance a, which may have allowed the finger pad to deform into the gap and have a greater contact area, which would result in a greater decrease in temperature. Likewise, the more-dense smaller spatial periods did not allow the finger pad to deform into the grooves to the same extent, and so may have resulted in a smaller temperature change. Although the contact

area on the top of each stimulus is the same for all stimuli (37.5 mm^2), it appears the finger pad was able to deform more around the textured surface and so in fact there was a larger contact interface. It is also important to understand the effect of contact force on the deformation of the finger when in contact with each surface. At higher contact forces, the finger pad would be expected to undergo more deformation against a flat surface. The first experiment showed that there was a rapid increase in contact area at low forces, and that over 70% of this change occurred at contact forces below 1 N. In this set of experiments, a contact force of 1 N was in used in all trials, which was presumably sufficient for the finger pad to conform to the geometry of the copper surface. At a contact force of 1 N, the finger did not penetrate into the textured array of the smoother surfaces, but would presumably do so at higher forces.

3.4 Conclusion

There was a progressive decrease in temperature as the spatial period of the truncated pyramids on the copper surface increased. Statistical analyses indicated that there was not a significant difference in the changes in temperature for the six surfaces tested, but there was a significant linear trend in the data. This suggests that there is a small but consistent decrease in skin temperature with increasing surface roughness for an object in contact with the hand. The experimental data did not confirm theoretical predictions, which may be due to the method used for estimating thermal contact resistance at lower forces.

4 Effect of Surface Roughness on Temperature Perception

The results from the previous experiment showed that there was a small change in temperature as a function of the surface roughness of the contact material. The objective of this experiment was to determine if the changes in temperature associated with the surface roughness of the object influenced the perceived coldness of the object in contact with the finger. Although the effect of surface roughness on the perception of temperature has not been previously evaluated, it has been shown that cooling the skin attenuates the perception of roughness (Green et al., 1979). Green showed that cooling the skin has an inhibitory effect on the perception of roughness, while warming the skin tended to improve the perception of roughness. In the present experiment, the surface roughness of two objects was varied, and participants were required to indicate which of the two surfaces felt cooler.

4.1 Method

Subjects. Ten normal healthy adults volunteered to participate in this study. There were six males, and four females ranging in age from 21 to 40 years old, with an average age of 26 years old. Five of the ten subjects participated in the previous study. The subjects had no known abnormalities of the tactile, proprioceptive, or thermal sensory systems and no history of peripheral vascular disease. The subjects reported that they were right handed. This research was approved by the MIT Committee on the Use of Humans as Experimental Subjects.

Apparatus. Two identical digital force gauges (Model DFS-20, SHIMPO) were mounted side by side on an aluminum frame as seen in Figure 4-1. The force gauges

were connected to a shielded connector block (NI BNC-2110, National Instruments), which was then connected to a data acquisition unit (NI DAQCard-6036E, National Instruments) and controlled by a Labview 8.5 program. Three thermistors were used to monitor the skin temperature on each finger and room temperature. The thermistors were connected to a separate data acquisition unit (Model 34970A, Agilent Technologies), and also controlled by a Labview program.

Composite fixtures were constructed to mount the copper test stimuli onto the force gauge. The fixtures consisted of an aluminum base (35 mm x 38 mm, 16mm thick) tapped with a M6 thread, with black opaque acrylic panels to obstruct the subject's view of the test stimuli. There was a slot in the back of each fixture to slide the copper stimuli in and out. The fixtures were numbered as 1 (left finger) and 2 (right finger).

Four copper test stimuli with spatial periods of 1.0, 1.5, 2.5, and 3.0 mm that were used in the previous experiment were chosen based on the measured temperature changes recorded in that experiment. The copper test stimuli were stored at room temperature, which was maintained at 23 °C.

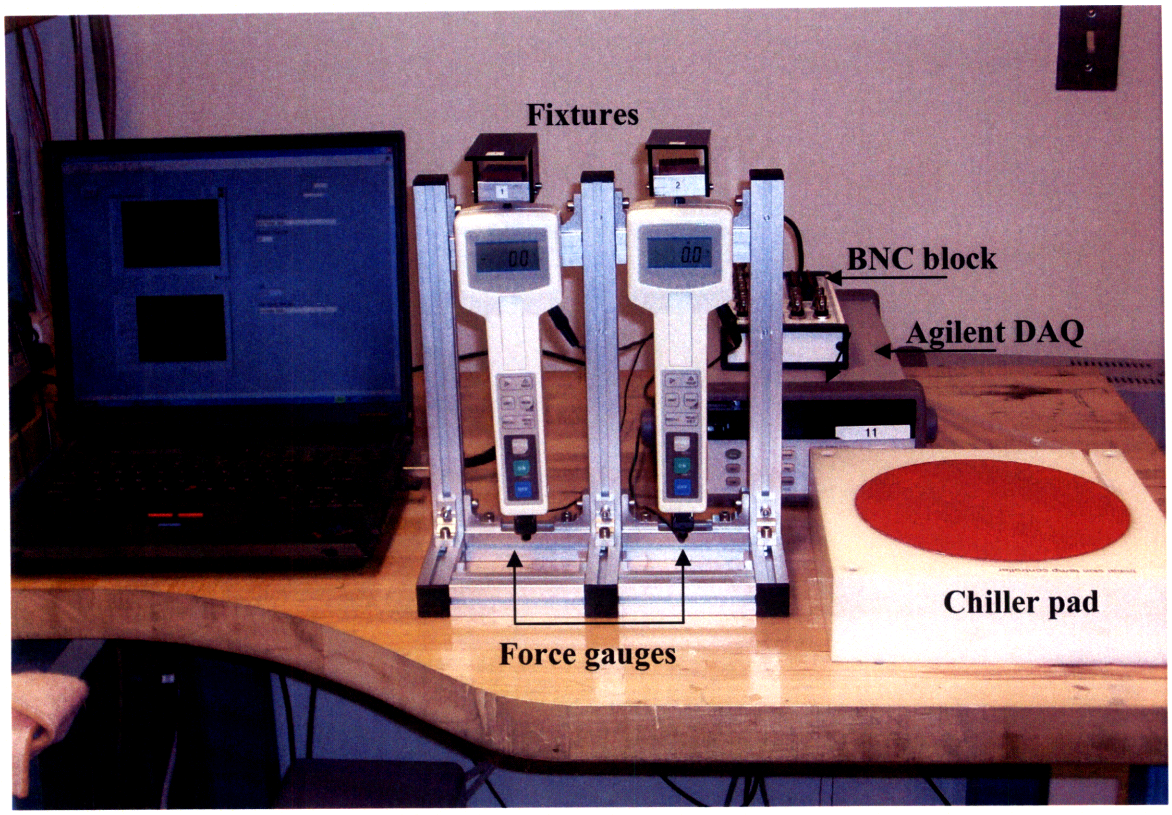

Figure 4-1. Experimental set-up for determining which of two copper test stimuli felt colder. Two fixtures with extended roofs are mounted on force gauges.

Procedure. Upon arrival, each subject's finger pad was cleansed with a cotton swab of isopropyl rubbing alcohol (70%) (CVS pharmacy). A thermistor was glued using a biocompatible cyanoacrylate (Liquid Bandage, Johnson & Johnson) on the side of the right and left index finger pads so as not to interfere with contact. Medical tape (Nexcare) was used to secure the thermistor leads along the hand and wrist. Subjects' initial skin temperatures ranged from 30.1 ºC to 36.8 ºC, with an average value of 34.1 ºC. The room temperature was maintained at 23 ºC as measured with a thermistor in free air.

Each of the four test stimuli was paired with the other stimuli including itself, which gave a total of 10 pairs. Five repetitions were completed per pair, which resulted

in 50 trials per subject. Within each block of 50 trials, the order of presentation of the test stimuli was randomized.

The subjects were presented with three auditory cues generated by a Labview 8.5 program. Subjects started with both hands on the chiller pad. At the first sound cue, they removed their hands from the chiller and placed their right and left index fingers in the holding position. At the second sound cue, subjects inserted their right and left index fingers into the fixtures and placed their fingers on the copper blocks. A two-alternative forced choice method was used in which the subjects were instructed to choose the cooler of the two surfaces by reporting which finger made contact with the cooler material, 1 (left) or 2 (right). The subjects were not told which spatial patterns were used, and no feedback was given as to the correctness of their judgments. They were encouraged to lift and replace their fingers on the test stimuli to sense the temperature, but were restricted from lateral scanning of the sample surface. A maximum presentation time of 10 seconds was given for each trial. At the third sound cue after 10 seconds, subjects removed their fingers from the test stimuli and placed them back on the chiller pad.

4.2 Results

A correct discrimination was defined as selecting the cooler, or rougher, of the two surfaces as defined by the results from the previous experiment. The results of this experiment are shown in Table 4.1.

Table 4.1. Percentage of correct discriminations

Spatial Period	1.0 mm	1.5 mm	2.5 mm	3.0 mm
1.0 mm	x	64.0	76.0	82.0
1.5 mm	x	x	70.0	80.0
2.5 mm	x	x	x	58.0
3.0 mm	x	x	x	x

The cells highlighted in green represent the discriminations that exceeded the threshold level of 72%, which was chosen as the level beyond which subjects could reliably discriminate between the two stimuli.

The overall change in temperature when the spatial period increased from 1 to 3 mm was 0.65 °C which is well above the threshold level. Participants were only able to reliably distinguish between 1 and 2.5 mm spatial period (ΔT= 0.49 °C), 1 and 3 mm (ΔT= 0.65 °C), and 1.5 and 3 mm (ΔT= 0.37 °C). Table 4.2 shows the difference in temperature between each stimulus pair averaged across 10 participants.

Table 4.2. Temperature difference between stimulus pairs

Spatial Period	1.0 mm	1.5 mm	2.5 mm	3.0 mm
1.0 mm	x	0.29 °C	0.49 °C	0.65 °C
1.5 mm	x	x	0.20 °C	0.37 °C
2.5 mm	x	x	x	0.17 °C
3.0 mm	x	x	x	x

The results of this experiment demonstrated that the small temperature differences measured in the previous experiment were perceptible when the difference in the spatial period of the copper surfaces exceeded 1.5 mm. The change in skin temperature through time was recorded in the previous experiment during the 10-second contact period. Figure 4-2 shows the change in skin temperature through time for the pairs of stimuli that subjects discriminated reliably in the present experiment. The rate of skin temperature change varied from 0.16 °C/sec to 0.23 °C/sec for the 1 mm and 3 mm spatial periods, respectively.

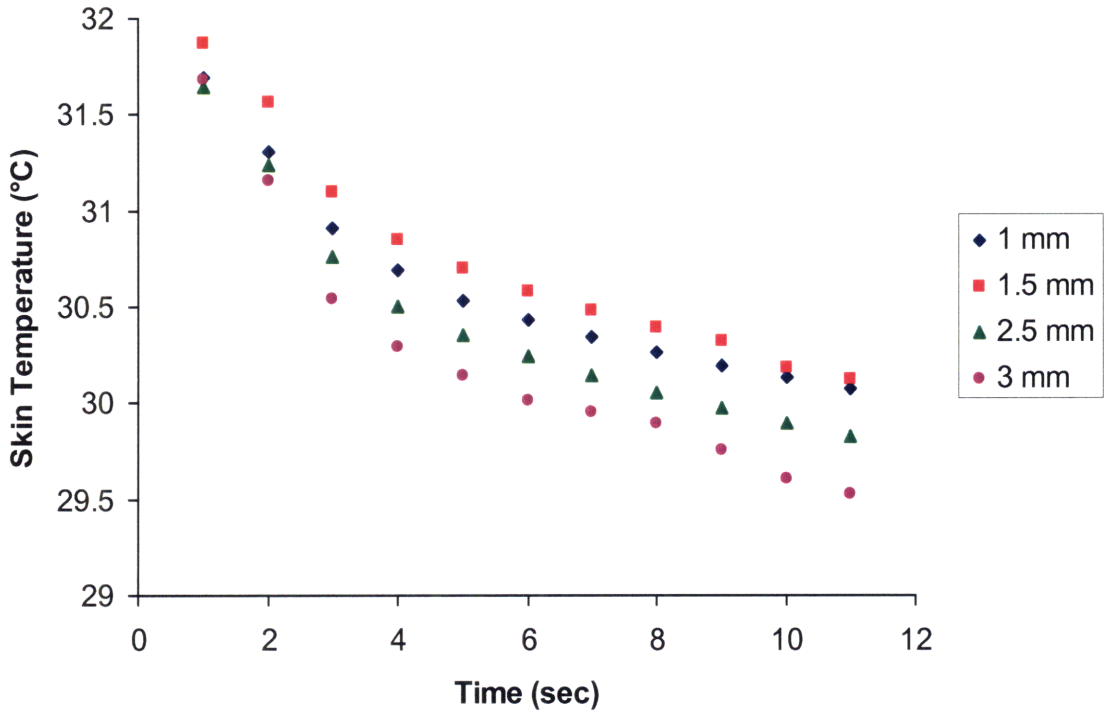

Figure 4-2. Skin temperature as a function of time averaged across 10 subjects.

The chance level for this experiment when the same stimulus was presented to both hands was 50%, and Table 4.3 shows that there was no systematic bias in the subjects' responses.

Table 4.3. Percentage of left and right hand selections for 10 subjects

Subject	% Left	% Right
1	75	25
2	45	55
3	80	20
4	20	80
5	70	30
6	35	65
7	50	50
8	55	45
9	50	50
10	20	80
Mean (%)	**50**	**50**

The mean was 50% for choosing the material in contact with the left and right fingers, which is expected when responding by chance.

4.3 Discussion

The ability of humans to discriminate changes in temperature are influenced by the site of stimulation, baseline temperature of the skin, and the amplitude and rate of the temperature change (Jones & Berris, 2002). If the rate of skin temperature changes very slowly, then an observer can be unaware of a temperature change of up to 5-6 °C, provided that the skin temperature remains within the neutral zone of 30-36 °C. If the change occurs at a more rapid rate, such as at 0.1 °C/sec, then it is possible to detect small increases and decreases in temperature as shown in Figure 4-3 (Kenshalo et al., 1968; Kenshalo, 1976).

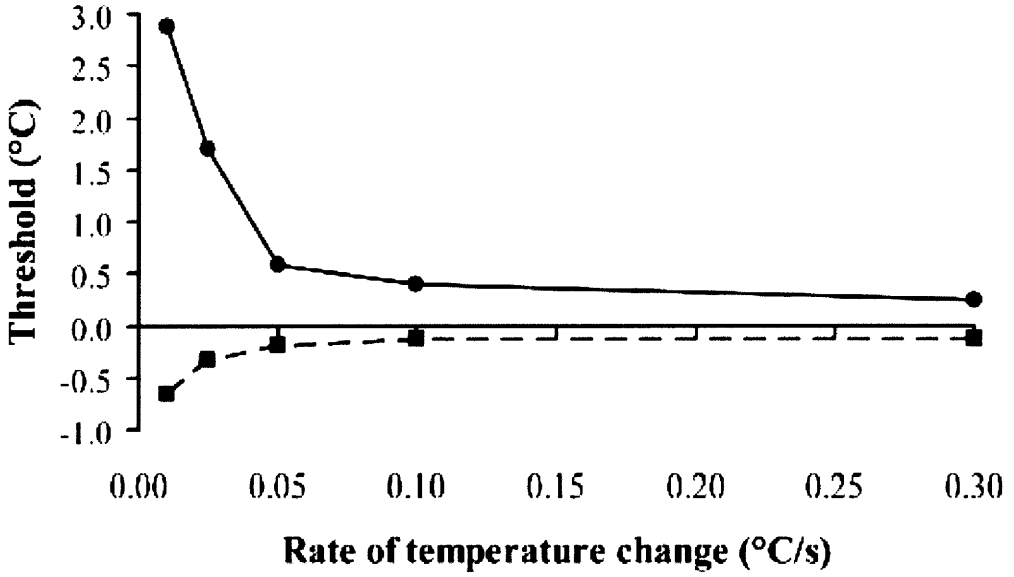

Figure 4-3. Warm (circles) and cold (squares) thresholds on the forearm as a function of the rate of temperature change at an adapting skin temperature of 32 °C (Kenshalo et al., 1968; Kenshalo, 1976).

The copper blocks were stored at room temperature (23 °C), and the initial skin temperatures of the subjects ranged from 30.1 °C to 36.8 °C, with an average temperature of 34.1 °C. The rate of temperature change based on the results from Experiment 2

ranged from 0.16 °C/sec to 0.23 °C/sec for spatial periods of 1 mm and 3 mm, respectively. Based on Kenshalo's (1976) data, the rate of temperature change in the present experiment was rapid enough to perceive the small temperature changes that resulted from varying the surface roughness of the material.

In this experiment, subjects used their right and left index fingers to perceive which of two stimuli was the cooler stimulus. Although the difference in skin temperature between all stimulus pairs as seen in Table 4.2 was above the cold threshold reported for the hand, 0.11 °C (Stevens & Choo, 1998), subjects were unable to reliably discriminate between all copper stimuli in the present task. A possible explanation may be due to the effects of spatial summation during simultaneous presentation. Thermal perception is characterized by spatial summation and poor spatial resolution. Spatial summation refers to an intensified perception of a stimulus as its spatial extent increases. Both warm and cold thresholds diminish when stimuli are presented symmetrically (Rozsa & Kenshalo, 1977).

The perceived magnitude of a cold thermal stimulus is a function of both the area of stimulation and its intensity. Both variables are equally important and can be traded to produce a given level of cold sensation. Although the contact area on the top of each copper stimulus is the same for all stimuli, it appears that the viscoelastic nature of the finger pad allowed it to deform more on the surfaces with larger spatial periods, so that there was a larger contact interface. The increased contact area provided a larger surface for heat to flow out of the finger to the copper surface, and therefore resulted in the rougher surfaces being perceived as cooler.

4.4 Conclusion

The changes in skin temperature when the hand makes contact with surfaces of varying roughness are perceptible, and demonstrate that the perception of surface roughness is not only influenced by changes in temperature, but in turn affects the perception of temperature. It is possible to reliably perceive the small differences in temperature that result from a change in the surface roughness of the contact material. These findings confirmed the results from the previous experiment, in that subjects reliably chose the rougher of the two materials as the cooler stimulus. The viscoelasticity of the skin permitted a greater contact area between the finger and copper surface at higher spatial periods, which allowed for a greater heat flux to be conducted out of the finger pad.

5 Effect of Object Temperature on Force Perception

Sensory feedback is used to control the manipulation of objects held in the hand. The object's physical properties are internally processed to scale the fingertip forces to the actual loading requirements. Sensory inputs from cutaneous mechanoreceptors influence the perceived magnitude of forces generated by individual fingers and the hand (Gandevia & McCloskey, 1977; Flanagan & Bandomir, 2000). Psychophysical studies suggest that the attributes of objects in contact with the skin interact perceptually, such that changes in one stimulus may alter the perception of others. Goodwin and Wheat (1992) found an effect of object curvature on the perceived contact force when spherical stimuli were passively applied to the finger tip. Increases in object curvature resulted in slight increases in the perceived contact force. Henningsen et al. (1995) conducted a series of experiments involving an active task which measured the ability to simultaneously match the forces generated by the right and left index fingers so that the forces were perceived to be identical, when the contact surface shape varied. Subjects consistently produced less force with the finger that pushed against the conical contact pad. These findings indicate that varying properties at the hand-object interface can distort the perception of the magnitude of applied force and the heaviness of weights due to the integration of tactile and proprioceptive inputs with signals arising from the centrally generated motor command.

Several other studies have examined the effect of skin anesthesia on force and weight perception, and in particular the loss of sensory inputs from cutaneous afferents from the thumb and index finger. When the skin on the thumb is anesthetized, the perceived heaviness of objects lifted by flexing the thumb increased by over 40%,

whereas the perceived heaviness increased by 13% for objects lifted with the anesthetized index finger (Kilbreath et al., 1997). Nowak et al. (2001) demonstrated that a lack of sensory feedback from the finger tips due to anesthesia resulted in a marked increase in grip forces during arm movements with a grasped object.

The objective of the final set of experiments is to determine whether the perception of contact force is affected by the surface temperature of the object in contact with the hand. Weber (1846) reported that a cold German coin felt approximately as heavy as two warm coins when placed on the forehead. He conjectured that cooling an object has an intensifying effect while warming has an attenuating effect on pressure sensation. It has since been shown that Weber's conjecture holds true for the intensifying effect of cold objects, but warmth can also intensify pressure sensation although the effect is considerably smaller and limited to certain body sites (Stevens & Hooper, 1982). A "reverse" Weber phenomenon has also been investigated, and there appears to be no effect of changing the force of stimulation on the sensation of warmth or cold (Zimmermann & Stevens, 1982). The final set of experiments utilizes thermal displays to simulate object temperatures and measures the subject's ability to match forces generated with their right and left fingers.

5.1 Method

Subjects. Ten normal healthy adults volunteered to participate in this study. There were seven males, and three females ranging in age from 21 to 40 years old, with an average age of 26 years old. The subjects had no known abnormalities of the tactile, proprioceptive, or thermal sensory systems and no history of peripheral vascular disease.

The subjects reported that they were right-handed. This research was approved by the MIT Committee on the Use of Humans as Experimental Subjects.

Apparatus. Two Peltier devices (Model DT6-6L, Marlow Industries Inc.) were used to display thermal stimuli to the fingers. Each Peltier device was positioned on top of a copper heat sink (30 mm x 30 mm x 5 mm), which was connected to a recirculating chiller (Model 1147P, VWR International). A thin layer of thermal grease (AOS non-silicone HTC) was applied between the copper heat sink and the Peltier device as seen in Figure 5-1.

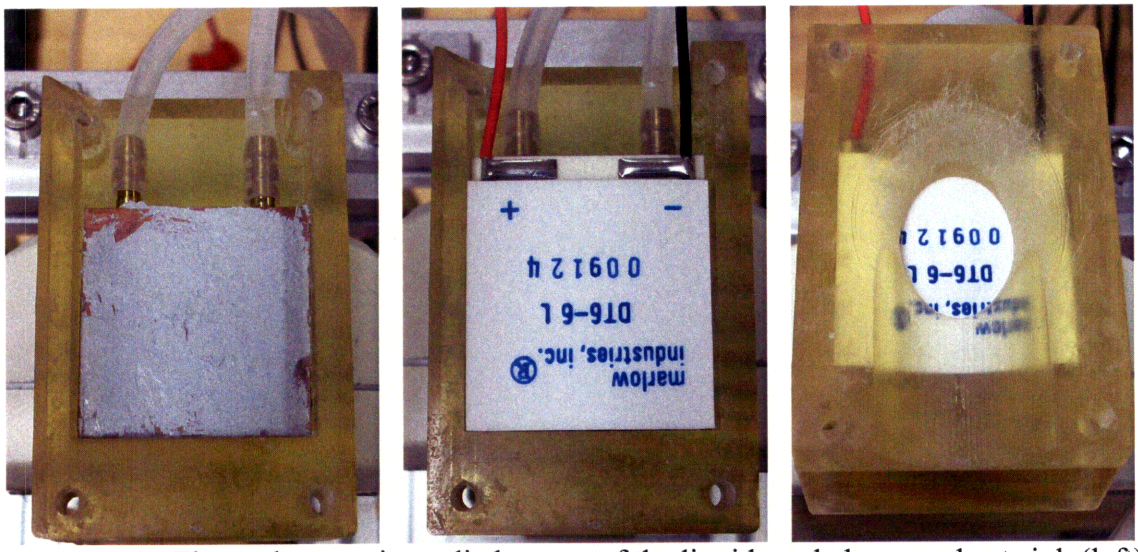

Figure 5-1. Thermal grease is applied on top of the liquid-cooled copper heat sink (left), and the Peltier device (middle) is compression-fitted inside the SLA fixture (right).

A three-piece fixture was designed to mount the Peltier device onto the copper heat sink, and was constructed with a rapid prototyping system (Viper Laser Stereolithography Forming Center, 3D Systems) as seen in Figure 5-2.

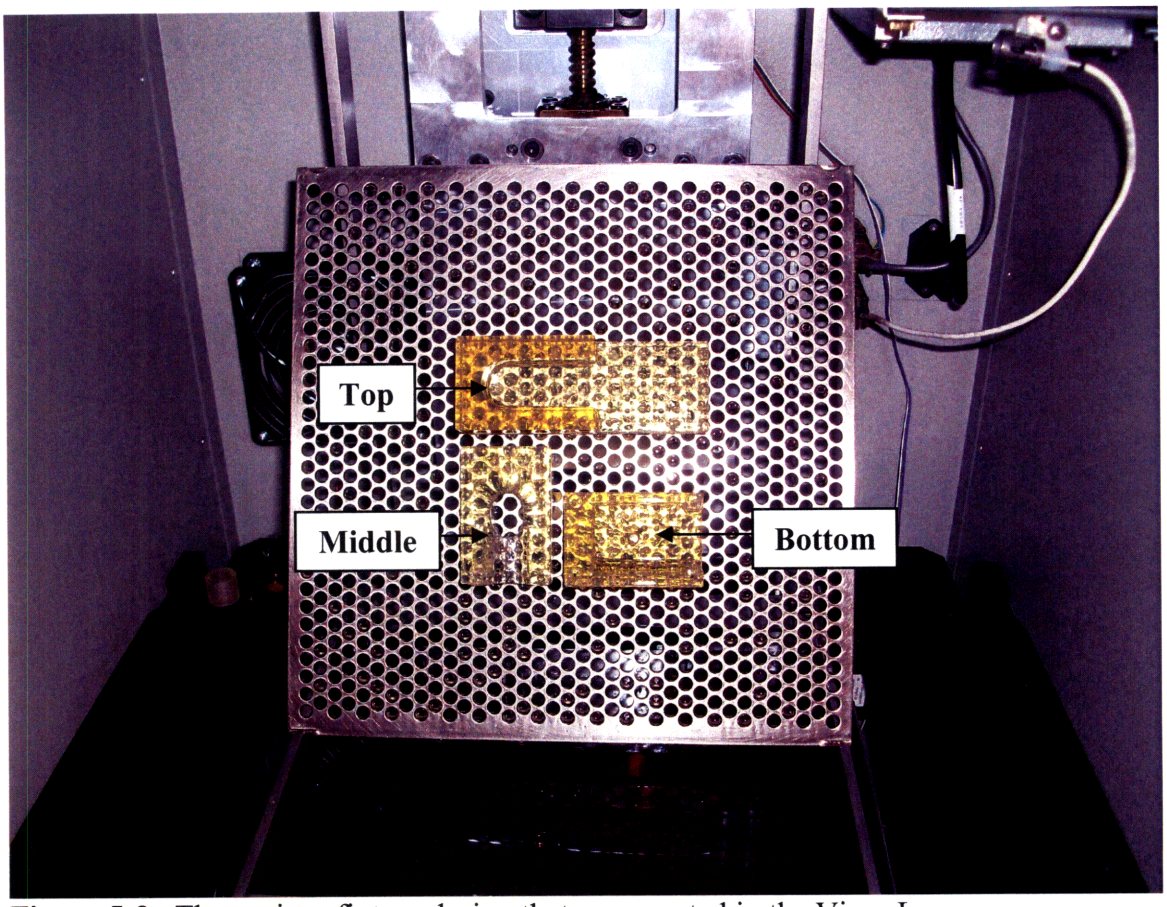

Figure 5-2. Three-piece fixture design that was created in the Viper Laser Stereolithography Forming Center.

The bottom piece of the fixture was 60 mm x 40 mm x 20 mm, and contained a slot (41 mm x 31 mm x 9 mm) to accommodate the Peltier device and copper heat sink. The middle piece of the fixture had an elliptical hole, with a primary axis of 10.5 mm, and a secondary axis of 7.5 mm, and was rounded to allow for comfortable finger insertion. The top piece of the fixture had a channel through which the index finger could be inserted, so that it could contact the Peltier device in the elliptical opening in the middle piece of the fixture. An extended roof was added to prevent subjects from visually assessing the forces applied by their fingers. The three pieces of the fixture were assembled with four M3 screws, and the bottom piece was threaded with an M6 hole to be mounted onto each force gauge as shown in Figure 5-3.

a.

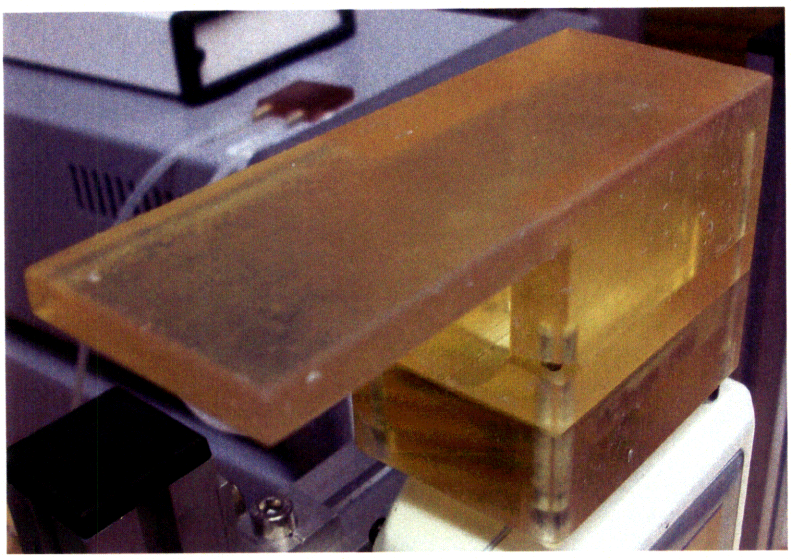

b.

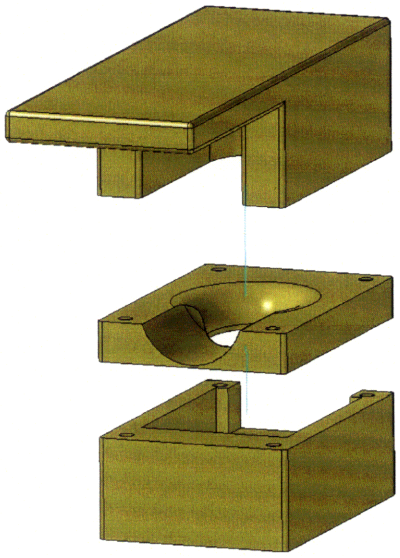

Figure 5-3. Fully assembled fixture with the Peltier device and copper heat sink installed (a) and an exploded assembly drawing of a fixture (b).

The fixtures were attached to two identical force gauges (Model DFS-20, SHIMPO), which were mounted side by side on an aluminum frame. The force gauges were zeroed when the weight of the fixture containing the Peltier and the heat sink was placed on it. The force gauges were connected to a shielded connector block (NI BNC-

2110, National Instruments), which was then connected to a data acquisition unit (NI DAQCard-6036E, National Instruments) and controlled by a Labview 8.5 program. Two thermistors were used to monitor the skin temperature on each finger, and three type E thermocouples were used to measure the surface temperature on the presentation side of each Peltier device and room temperature. The thermocouples mounted on the Peltier devices provided temperature feedback to the PI controller in the Labview program. The thermocouples were connected to a separate data acquisition unit (Model 34970A, Agilent Technologies). Two power supplies (Model E3632A, Agilent Technologies) were used to provide voltage and current to the Peltier devices. The temperature control flow chart is shown in Figure 5-4.

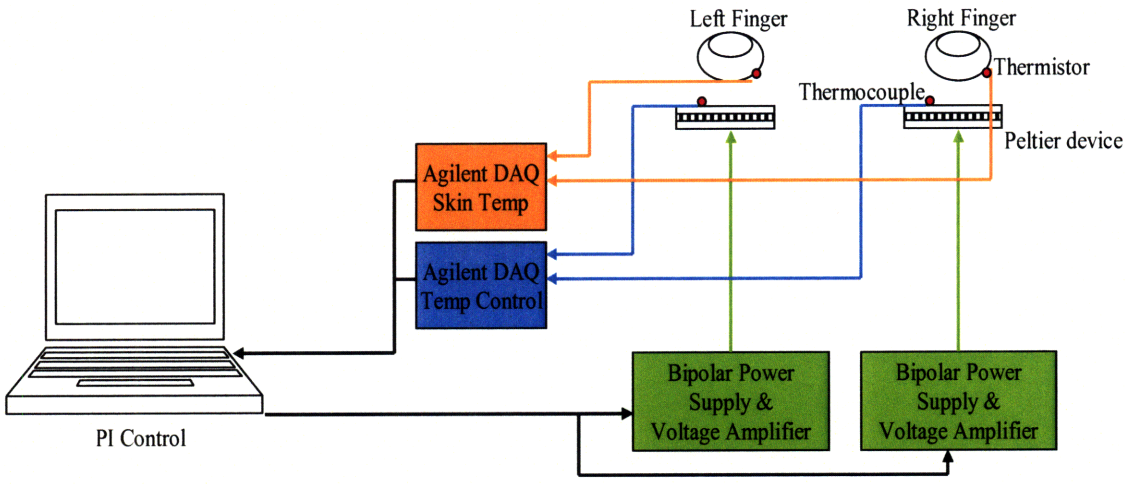

Figure 5-4. Schematic representation of temperature control of thermal displays.

Another recirculating chiller (Model 1167P, VWR International) as described in Chapter 2, provided a surface to maintain the skin temperature at 32 °C at the start of the experiment, and between trials prior to making contact with the Peltier devices. The room temperature was maintained at approximately 22 °C for the duration of each experiment. The experimental set-up is shown in Figure 5-5.

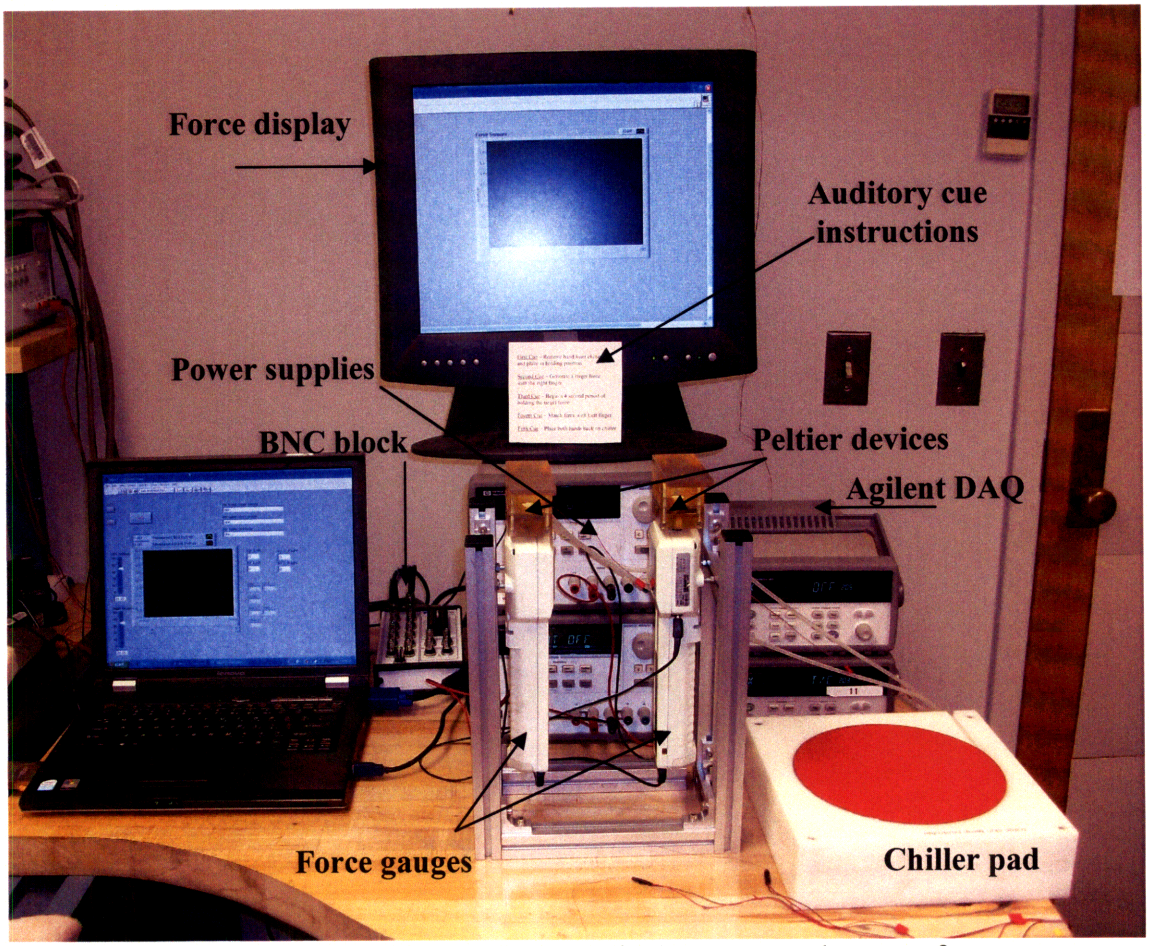

Figure 5-5. Experimental set-up with thermal displays mounted on two force gauges.

Procedure. Upon arrival, each subject's right and left index finger pads were cleansed with a cotton swab of isopropyl rubbing alcohol (70%) (CVS pharmacy). Thermistors were glued using a biocompatible cyanoacrylate (Liquid Bandage, Johnson & Johnson) on the index finger pads on the perimeter of the contact area. Baking soda was used to

mark the contact area of the finger pad at a force of 8 N, and the thermistor was glued on the edge of that contact area. Medical tape (Nexcare) was used to secure the thermistor leads along the hand and wrist.

Subjects were presented with auditory cues generated by the Labview program, which indicated the sequence of the experiment. Subjects began with their right and left hands on the chiller pad until their skin temperature reached 32 °C as measured by the thermistors on the finger pads. At the first sound cue, subjects removed their hands from the chiller pad and placed it in a holding position. At the second sound cue, subjects were instructed to generate a given force with their right index finger on the Peltier device, which was set to a specific temperature. The reference, or right-handed, Peltier device was set to one of three warm temperatures (34, 36, 38 °C), or three cool temperatures (22, 24, 26 °C), or a neutral temperature (32 °C). A display showed the target force and the measured force for the right index finger, and the subject was given 2 seconds to match the target force. The third sound cue signaled the start of a 4-second time period during which the subject was instructed to hold the target force and attend to the sensation associated with that target force. The fourth sound cue signaled the subject to place their left index finger on the other Peltier device, which was maintained at a neutral temperature of 32 °C, and to produce a force that matched the perceived magnitude of the force being produced by the right index finger. They were given 3 seconds to match the forces. No feedback was provided about the force produced by the left index finger. At the fifth sound cue, the subject moved both hands back onto the chiller pad. The next trial began when the subject's skin temperature returned to 32 °C.

The target forces used in this experiment were 1, 2, 4, 6, and 8 N. A Labview program recorded the skin temperature data at a sampling frequency of 4 Hz, which was sufficient to capture the change in temperature. The force data was sampled at 55 Hz. Each of the five target forces was paired with seven contact surface temperatures, which gave a total of 35 pairs. Two repetitions were completed per pair, which resulted in 70 trials per subject. The order of presentation of warm and cool stimuli was randomized among subjects.

5.2 Results

The matching force was determined from the average force applied for 1 second during the middle of the 3-second matching time interval for each subject at each force. The selected timeframe captured the matching force after the initial force generation. The matching forces under the neutral condition (32 °C) as a function of the reference forces are shown in Figure 5-6. A linear regression function fitted to the data accounted for 99% of the variance. The slope of the regression line indicates that subjects slightly overestimated low forces and consistently underestimated higher reference forces, and were most accurate in the middle of the range of forces presented.

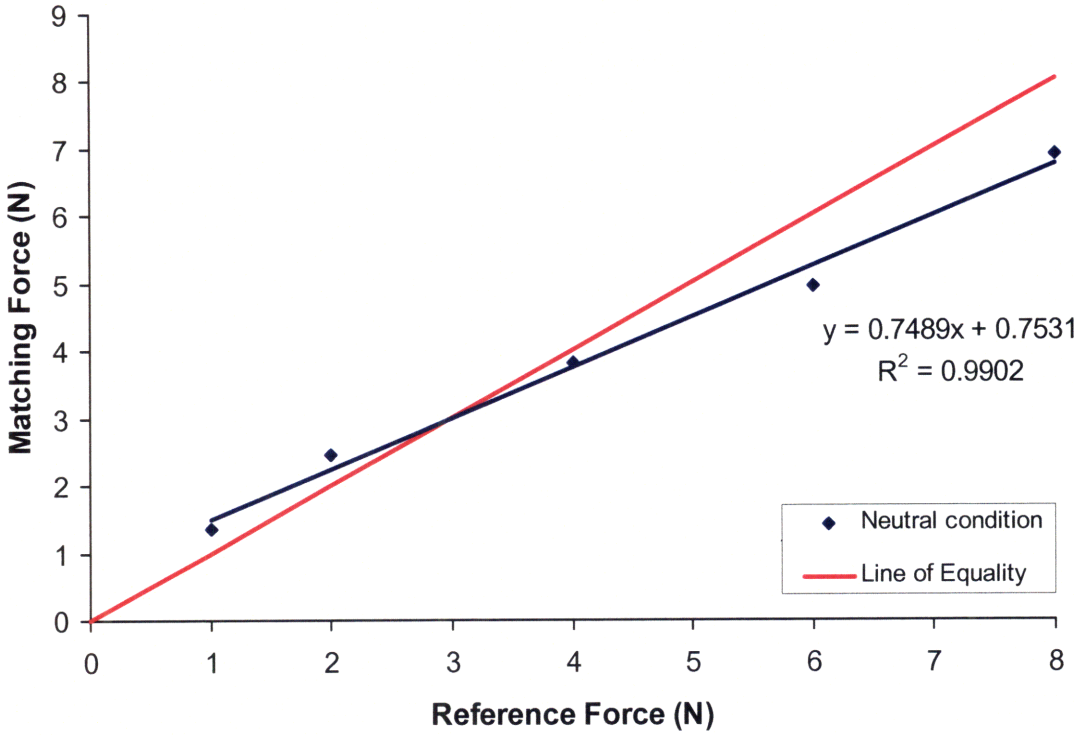

Figure 5-6. Matching force as a function of reference force for the neutral condition averaged across 10 subjects. A line of equality (matching equals reference force) is shown in red.

Figure 5-7 shows the matching force as a function of the reference force for the cool and neutral surface temperatures. Linear regression functions fitted to the data accounted for 99% of the variance for all cool stimuli presented. The slopes of the regression lines were not significantly different as the surface temperature changed. The slopes ranged from 0.78 for the 22 °C surface temperature, 0.68 for the 24 °C surface, and 0.85 for the 26 °C surface. Similarly, the slopes of the regression lines for the warm stimuli were 0.78 for the 34 °C surface, 0.80 for the 36 °C surface, and 0.76 for the 38 °C surface. Linear regression functions fitted to the warm surface temperatures accounted for 99% of the variance as seen in Figure 5-8.

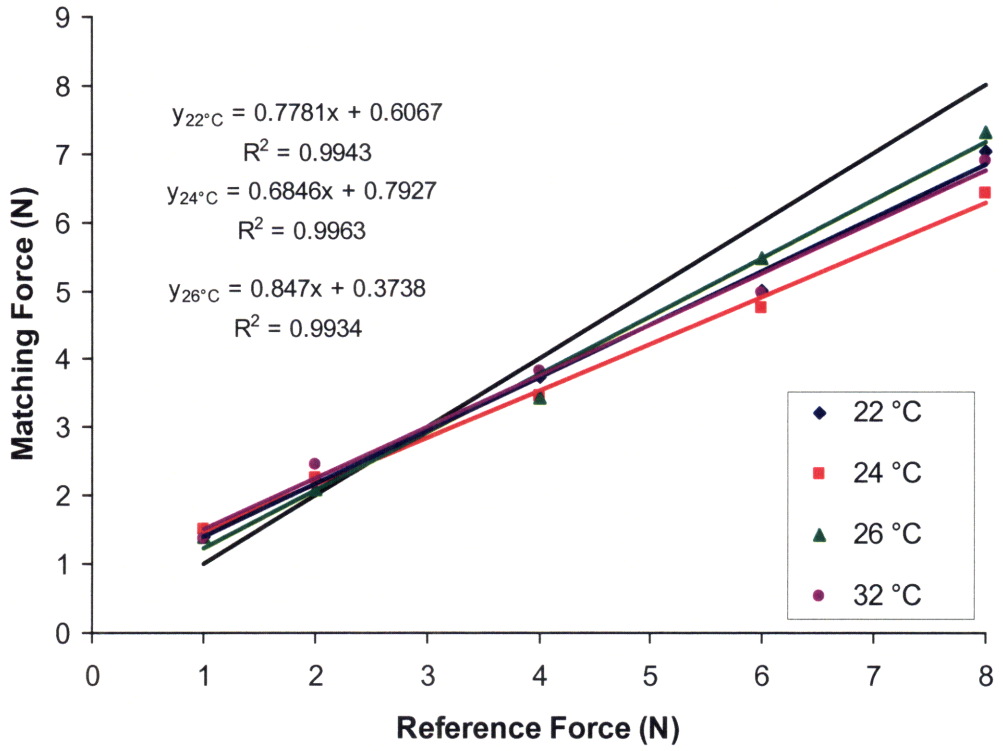

Figure 5-7. Matching force as a function of reference force for cool and neutral stimuli averaged across 10 subjects. A line of equality is shown in black.

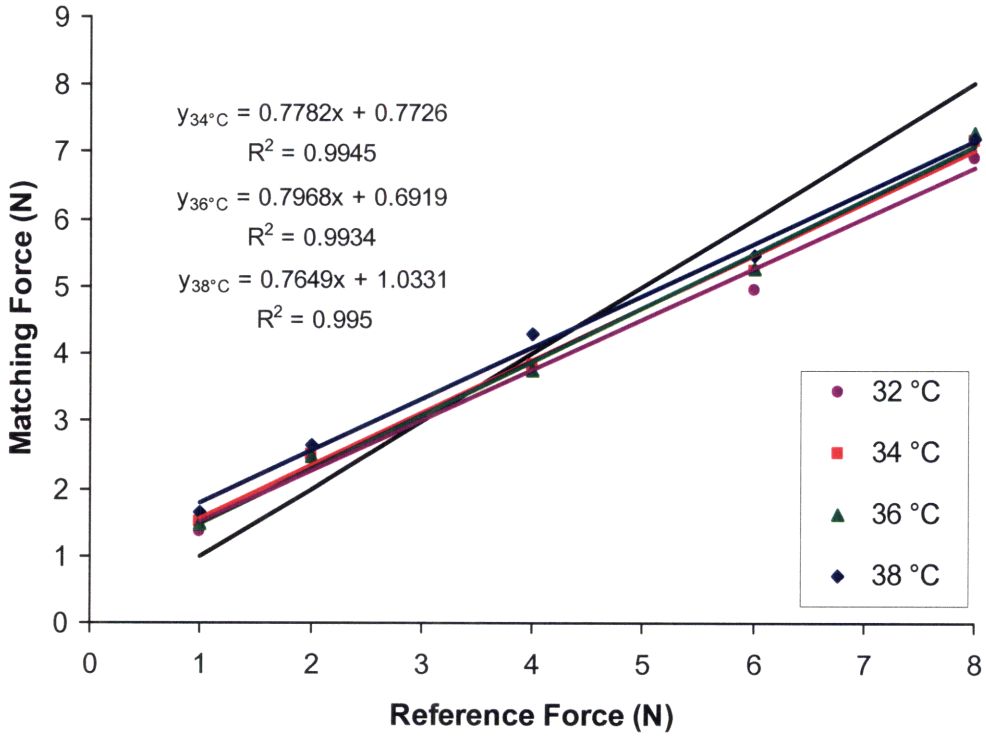

Figure 5-8. Matching force as a function of reference force for warm and neutral stimuli averaged across 10 subjects. A line of equality is shown in black.

The matching forces averaged across 10 subjects are plotted as a function of surface temperature for the cool and neutral stimuli in Figure 5-9 and for the warm and neutral stimuli in Figure 5-10. Figure 5-11 displays the matching forces as a function of surface temperature for all stimuli.

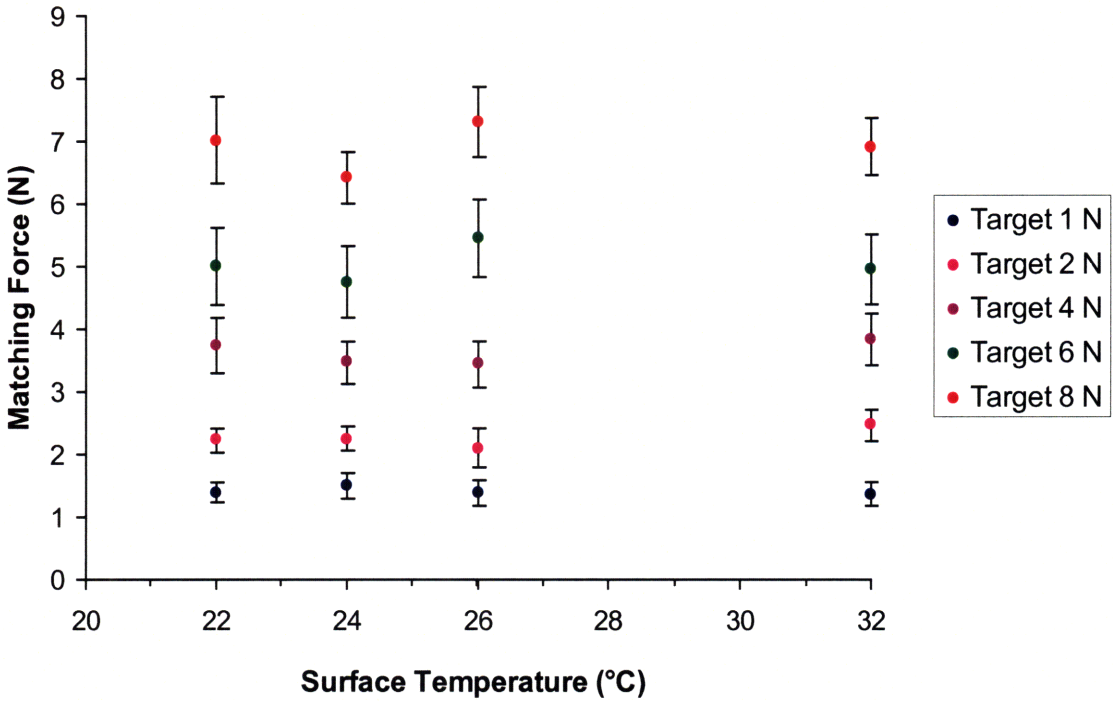

Figure 5-9. Matching force for cool and neutral stimuli as a function of reference finger surface temperature. The standard errors of the mean are shown.

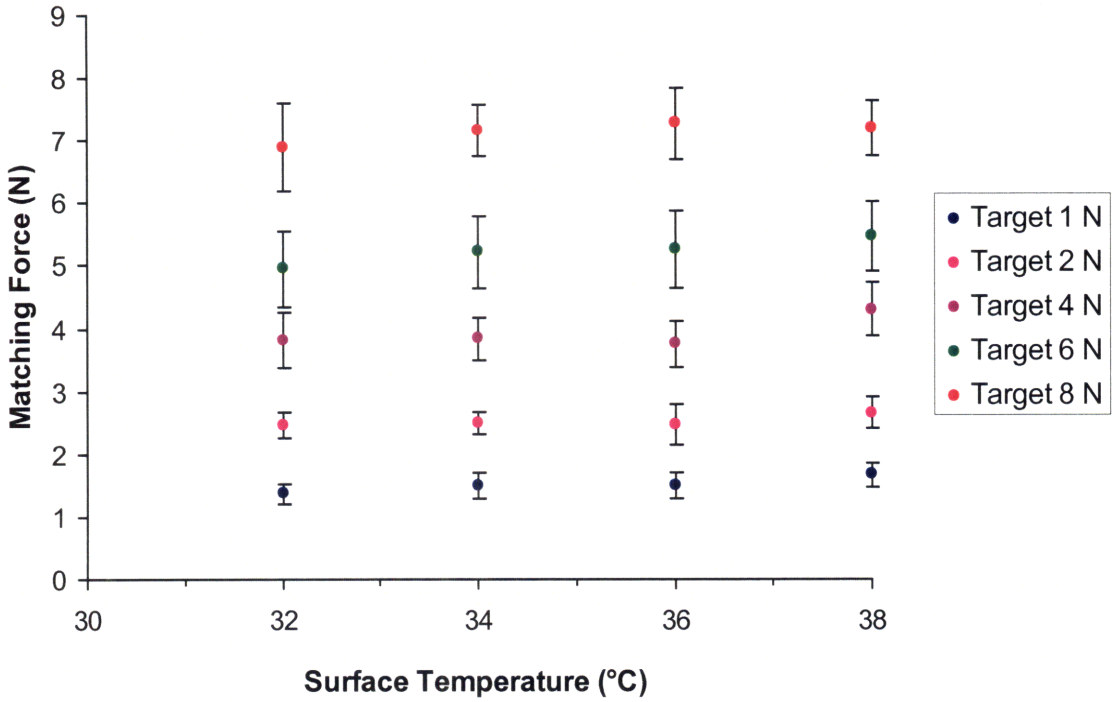

Figure 5-10. Matching force for warm and neutral stimuli as a function of reference finger surface temperature. The standard errors of the mean are shown.

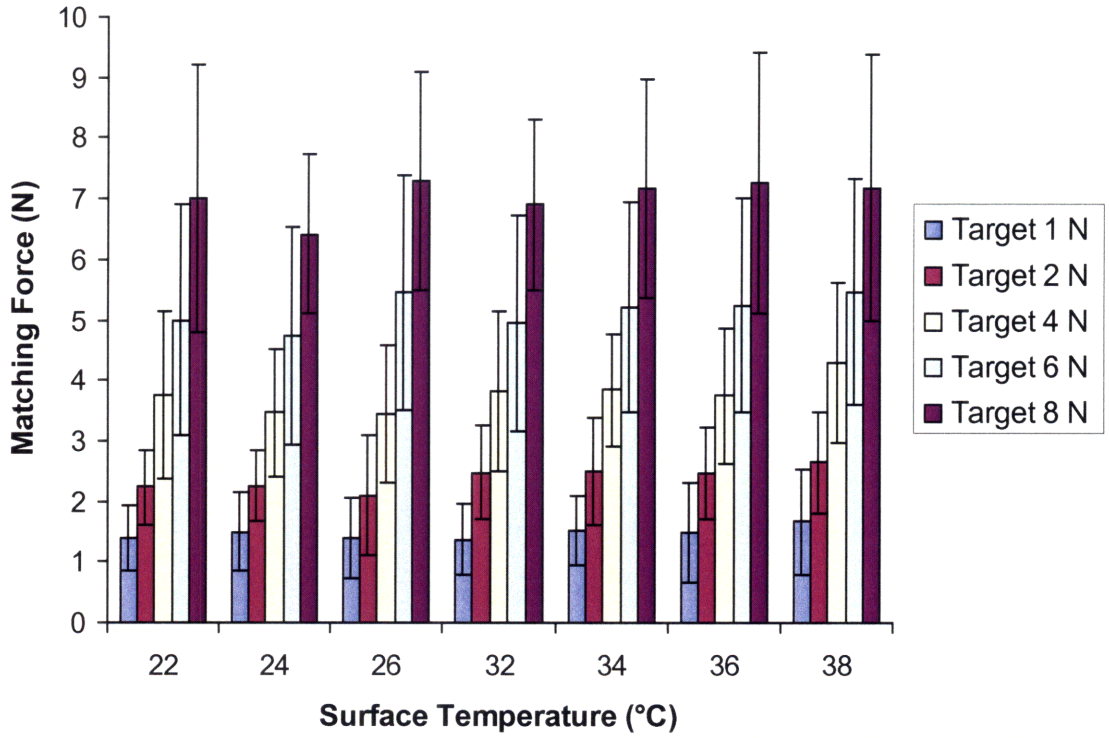

Figure 5-11. Left finger match force is shown as a function of reference surface temperature for all stimuli. The standard deviations are shown.

A repeated-measures ANOVA with the reference force and surface temperature as the within factors and matching force as the dependent variable indicated that there was a significant difference in the matching force as a function of reference force ($F(1, 12)= 125.36$, $p< 0.001$), but there was not a significant difference as a function of reference surface temperature ($F(4, 39)= 1.35$, $p= 0.267$) with Huynh-Feldt corrected df and the interaction was not significant.

5.3 Discussion

Neural signals delivered to the relevant motoneurones trigger a muscle to contract, which in turn produces an isometric force or causes movement about a joint. The final force developed by the muscle depends on the voluntarily-generated central motor command, in addition to signals related to reflex facilitation or inhibition provided by peripheral inputs (Gandevia & McCloskey, 1977). Alterations of cutaneous and joint afferent input can influence the perception of force (Kilbreath et al., 1997). Gandevia and McCloskey (1977) showed that the perceived heaviness of a weight lifted by flexion of the thumb increased when the digital nerves of the thumb were anesthetized. The effect of skin anesthesia on force and weight perception is thought to reflect the loss of the net facilitatory effect of the reflex input from cutaneous and joint afferents on the magnitude of the descending motor command. The mechanisms underlying the generation of force suggest that other sensory inputs such as thermal cues may influence force perception.

Stevens and Hooper (1982) performed a series of experiments using passive touch in which weights were placed on a subject's forearm and the effect of skin and object

temperature on weight perception was studied. Subjects made magnitude estimations of the apparent weight of circular aluminum stimulators of varying mass and temperature. The stimuli were set to cold (0 °C), neutral (34 °C), and warm (45 °C) temperatures as regulated by a water bath, and were then placed on the forearm where the skin was maintained at 25, 33, or 38 °C. The stimulators weighed 21, 45, and 105 g (0.20, 0.44, 1.0 N) with a surface area equal to 12.6 cm^2, corresponding to contact pressures of 0.16, 0.35, 0.82 kPa. The contact pressures for the finger pad in the present experiment ranged from 7.2 to 45.5 kPa, corresponding to contact forces of 1 N and 8 N, respectively. Although the contact pressure range is considerably lower in Stevens and Hooper's (1982) experiments and the site of stimulation is different, the results are relevant to the present findings. Stevens and Hooper (1982) showed that under neutral skin conditions, cold objects felt heavier than neutral ones, and warm objects felt somewhat heavier, indicating that the sensation of weight is amplified as the object temperature increases or decreases. The results from the present experiment on the finger pad did not reveal this differentiation, in that the temperature of the contact surface did not have a significant effect on force perception over the range of 22 to 38 °C. The difference in findings may be due to the active nature of force production in the present experiment as well as the range of temperatures selected, where the coldest surface temperature presented was 22 °C, as compared to 0 °C in Stevens and Hooper's experiments. Also, the warmest surface in the present experiment was 38 °C, whereas the warmest object in their experiment was 45 °C, which is at threshold for the onset of pain.

Stevens and Hooper (1982) also explored how skin temperature and object temperature combine to produce thermal sensation. They showed that both warming and

cooling the skin eliminated the intensifying effect of warm objects. However, warming the skin did not change the intensifying effect of cold objects, and cooling the skin only slightly diminished the intensifying effect of cold objects. Their findings show that cold has a larger and more robust impact on apparent weight than warmth. In the present experiment, the skin temperature was maintained at a neutral temperature of 32 °C, so that only the effect of object temperature could be evaluated.

Irrespective of temperature effects, some regions of the body are more sensitive to pressure than others. Stevens (1979) explored the effect of the site of stimulation on thermal sensation. The same circular object stimuli were judged to feel heavier on the palm of the hand than on the back. These results confirmed Weber's (1834) proposed correlation between weight sensitivity and tactile acuity. Stevens (1982) conjectured that if weight perception and tactile acuity are mediated by the same receptor network, then temperature may influence apparent weight and tactile acuity. He reported that cooling and warming objects in contact with the skin on the forearm caused a marked improvement in the skin's tactile acuity relative to thermally neutral stimulation.

Psychophysical experiments on tactile perception have been conducted using both active and passive stimulation. During active touch, the observer initiates and controls the acquisition of sensory information, whereas in passive touch, the stimulus is brought into contact with the observer. Gibson (1962) conducted a series of experiments that demonstrated reduced tactile pattern recognition during passive exploration. These results may be attributed either to difficulty in reproducing an active task, where other tactile and thermal inputs (such as contact force, duration, and area) are available to the observer, or to a difference in the sensory neural mechanisms underlying active and

passive touch. Vega-Bermudez et al. (1991) performed several tactile letter recognition experiments where the inputs for passive and active touch were virtually identical. The direction and range of motion, contact time, and orientation of stimuli were controlled. There was not a statistically discernible difference between active and passive touch for tactile letter recognition. The effects of active versus passive touch remains an important question in the literature.

Flanagan and Bandomir (2000) conducted an experiment using active exploration, which examined the effect of changes in grasp configuration on the perceived heaviness of objects in a weight discrimination task. Subjects compared the weights of a series of test objects with the weight of a reference object using a set of pre-defined grasping configurations. Objects were perceived to be lighter when lifted with a larger contact area, wider grip, and five digits in comparison to two digits. They showed that changes in the voluntarily-generated central motor commands associated with grasp difference may influence perceived weight. Their study did not take into account the object's material properties or thermal characteristics, which also may have contributed to the perceived weight of the stimuli.

5.4 Conclusion

The parameters that were varied in this experiment included object temperature (cold, neutral, and warm) and contact force. Varying the object temperature did not have a significant effect on force perception over the range of temperatures evaluated from 22 to 38 °C. A larger range of object temperatures may be needed to demonstrate the influence of sensory inputs from cutaneous mechanoreceptors on the perceived magnitude of finger forces.

6 Conclusions

6.1 Summary and Contributions

The goal of this thesis was to evaluate the influence of contact conditions on the thermal response of the skin and their perceptual effects in hand-object interactions. Several aspects of contact were examined including contact force, surface temperature, and surface roughness. All of the tasks involved active haptic exploration, and the skin was maintained at a neutral temperature for all experiments. The thermal response of the finger pad was measured with thermistors for local transients, as well as with infrared imaging to gain information about the temperature distribution across the finger pad in different hand-object scenarios. A series of experiments evaluated the thermal response of the skin from both physiological and psychophysical perspectives.

The first experiment was conducted to determine the effect of contact pressure on the change in skin temperature. Subjects generated a target force ranging from 0.1 to 6 N, which encompasses the range of forces used in hand-object manipulation. The temperature of the finger pad was measured with both a thermistor on the edge of the contact area, as well as with an infrared camera. The decrease in skin temperature was found to be greater when averaged across the entire contact area in the infrared image. These results were compared to predicted values from the thermal model proposed by Ho and Jones (2006a). The model accurately predicted skin temperature change at higher contact pressures (greater than 12 kPa), but underestimated values at lower contact forces. The difference between the theoretical predictions and the experimental results may be due to the estimation of thermal contact resistance at low contact pressures.

Although it is known that the surface roughness of an object affects the change in skin temperature upon contact, this effect had not been previously quantified. Highly conductive copper surfaces were machined with truncated pyramids of varying spatial period from 0.8 mm (smooth) to 3 mm (coarse). The contact force and duration were held constant, while the temperature change was measured with a thermistor on the edge of the contact area. The overall change in temperature was 0.54 °C as the spatial period increased from 0.8 mm to 3 mm. Although relatively small temperature changes were measured, greater heat transfer may have occurred that could not be captured due to the limitations of a local contact temperature sensor. Statistical analysis revealed there was a significant linear trend, which suggests there is a small but consistent decrease in skin temperature as the spatial period increases. Interactions between the thermal and tactile sensory signals may reflect mechanical changes at the skin-object interface. It may be necessary to account for the geometry of the surfaces in contact, in addition to the RMS surface roughness and asperity slope, when determining thermal contact resistance. The previous two sets of experiments indicate that both contact pressure and surface roughness influence the change in skin temperature when the hand is in contact with an object.

The objective of the third experiment was to determine the perceptual effects of the relatively small changes in temperature that were caused by varying surface roughness. A two-alternative forced choice method revealed that subjects could reliably discriminate between copper stimuli on the basis of thermal cues when the difference in the spatial periods was 1.5 mm or greater, even though the temperature differences were small. As the stimulus became rougher, subjects perceived the surface to be cooler. The

changes in temperature due to varying surface roughness are perceptible, and demonstrate that the perception of surface roughness is not only influenced by changes in temperature, but in turn affects the perception of temperature.

The fourth set of experiments sought to investigate the effect of varying the object's temperature on the perception of contact force. Two thermal displays were designed with a PI control to display cool, neutral, and warm temperatures to the finger pad. Force feedback was given for the reference finger, and no feedback was given as to the force applied by the matching finger. The surface temperature of the object did not have a significant effect on the perceived magnitude of force over the range that was examined. It would be useful to examine a wider range of object temperatures at different contact durations to confirm these initial findings.

In summary, this thesis characterized important factors that affect the thermal response of the hand during contact. The results of these experiments may be incorporated into future thermal models in an effort to create more realistic thermal and haptic displays for virtual environments and teleoperated systems.

6.2 Future Work

The influence of contact pressure on the thermal response of the skin can be predicted at higher values with the Ho and Jones thermal model (2006a) as shown in Experiment 1. However, the estimation of thermal contact resistance (Yovanovich, 1981) is not adequate to predict temperature changes at lower contact pressures. It would be useful to develop a new model of thermal contact resistance, and design a set of experiments to validate the effects of thermal contact resistance at low contact pressures. The change in temperature due to contact pressure is also attributed to the collapse of

capillary blood vessels in the finger tip. A fluid flow model describing the extent of vasoconstriction (or vasodilation for warming stimuli), as well as the location of collapse (proximal or distal) may help to design thermal displays that would more accurately simulate virtual objects.

All of the experiments in this thesis involve active exploration of stimuli. Thermal effects may vary depending on whether the stimuli being processed are primarily tactile or proprioceptive in nature. It would be interesting to repeat the perceptual experiments with passive stimulation. In addition, the experiments were all designed to maintain the skin temperature thermally neutral. Initial skin temperature is a key factor in thermal modeling, and it would be useful to conduct a set of experiments in which the skin is initially warmed or cooled, and study the thermal response and perception of external stimuli under varying contact conditions. The ambient conditions for all of the experiments in this thesis were kept at the same temperature and relative humidity. Some applications of haptic devices, such as teleoperated robotic systems, may exist in different environments, and it will be necessary to model the temperature response of the skin under more extreme ambient conditions, such as underwater or in outer space.

References

Benali-Khoudja, M., Hafez, M., Alexandre, J.M., Benachour, J., Kheddar, A. (2003). "Thermal feedback model for virtual reality," *Proceedings of the International Symposium on Micromechatronics and Human Science*, 153-158.

Bergamasco, M., Alessi, A.A., Calcara, M. (1997). "Thermal feedback in virtual environments," *Presence*, 6: 617-629.

Citerin, J., Pocheville, A., Kheddar, A. (2006). "A touch rendering device in a virtual environment with kinesthetic and thermal feedback," *Proceedings of the IEEE International Conference on Robotics and Automation*, 3923-3928.

Connor, C.E., Hsiao, S.S., Phillips, J.R., Johnson, K.O. (1990). "Tactile roughness: neural codes that account for psychophysical magnitude estimates," *The Journal of Neuroscience*, 10(12): 3823-3836.

Darian-Smith, I. (1984). "Themal sensibility," *Handbook of Physiology: The nervous system*, Darian-Smith, I. (Ed.). Bethesda, MD: American Physiological Society, 879-913.

Darian-Smith, I., Johnson, K.O. (1977). "Thermal sensibility and thermal receptors," *Journal of Investigative Dermatology*, 69: 146-153.

Dellon, E.S., Keller, K., Moratz, V., Dellon, A.L. (1995). "The relationships between skin hardness, pressure perception and two-point discrimination in the fingertip," *The Journal of Hand Surgery*, 20: 44-48.

Deml, B., Mihalyi, A., Hanning, G. (2006). "Development and experimental evaluation of a thermal display," *Proceedings of 2006 EuroHaptics Conference*, 257-262.

Dépeault, A., Meftah, el-M., Chapman, C.E. (2008). "Tactile speed scaling: contributions of time and space," *The Journal of Neurophysiology*, 3: 1422-1434.

Dionisio, J., Henrich, V., Jakob, U., Rettig, A., Ziegler, R. (1997). "The virtual touch: haptic interfaces in virtual environments," *Computer and Graphics*, 21: 459-468.

Fedasyuk, D. (2003). "Thermal modeling of microelectronic equipment taking into account thermal contact conductance," *CADSM'2003*, Lviv-Slasko, Ukraine, 319-320.

Flanagan, J.R., Bandomir, C.A. (2000). "Coming to grips with weight perception: effects of grasp configuration on perceived heaviness," *Perception & Psychophysics*, 62: 1204-1219.

Gandevia, S.C., McCloskey, D.I. (1977). "Changes in motor commands, as shown by changes in perceived heaviness, during partial curarization and peripheral anaesthesia in man," *The Journal of Physiology*, 272: 673-689.

Gardner, E.P., Martin, J.H., Jessel, T.M. (2000). "The bodily senses," *Principles of Neural Science*, In Kandel, E.R., Schwartz, J.H., Jessel, T.M. (Eds.). 4th Ed. New York: McGraw-Hill, Health Professions Division, 430-449.

Gibson, J. J. (1962). "Observations on active touch," *Psychological Review*, 69: 477-49.

Goodwin, A.W., Wheat, H.E. (1992). "Magnitude estimation of contact force when objects with different shapes are applied passively to the fingerpad," *Somatosensory and Motor Research*, 9: 339-344.

Green, B., Lederman, S.J., Stevens, J.C. (1979). "The effect of skin temperature on the perception of roughness," *Sensory Processes*, 3: 327-333.

Greenspan, J.D., Kenshalo, D.R. (1985). "The primate as a model for the human temperature- sensing system: 2. Area of skin receiving thermal stimulation," *Somatosensory Research*, 2: 315-324.

Hardy, J.D., Oppel, T.W. (1937). "Studies in temperature sensation III. The sensitivity of the body to heat and the spatial summation of the end organ responses," *Journal of Clinical Investigation*, 16: 533-540.

Harrison, J.L.K., Davis, K.D. (1999) "Cold-evoked pain varies with skin type and cooling rate: A psychophysical study in humans," *Pain*, 83: 123-135.

Hedin, D.S., Seifert, G.J., Dagnelie, G., Havey, G.D., Knuesel, R.J., Gibson, P.L. (2006). "Thermal imaging aid for the blind," *Proceedings of the 28th IEEE EMBS Annual International Conference*, New York City, USA, 4131-4134.

Henningsen, H., Ende-Henningsen, B., Gordon, A.M. (1995). "Contribution of tactile afferent information to the control of isometric finger forces," *Experimental Brain Research*, 105: 312-317.

Ho, H., Jones, L.A. (2006a). "Thermal model for hand-object interactions," *Proceedings of the IEEE Symposium on Haptic Interfaces for Virtual Environment and Teleoperator Systems*, 461-467.

Ho, H., Jones, L.A. (2006b). "Contribution of thermal cues to material discrimination and localization," *Perception & Psychophysics*, 68: 118-128.

Ho, H., Jones, L.A. (2007). "Infrared thermal measurement system for evaluating model-based thermal displays," *Second Joint EuroHaptics Conference and Symposium on*

Haptic Interfaces for Virtual Environment and Teleoperator Systems (WHC 2007), Tsukuba, Japan, 157-163.

Ho, H., Jones, L.A. (2008). "Modeling the thermal responses of the skin surface during hand-object interactions," *Journal of Biomechanical Engineering*, 130(2): 21005-1-8.

Hollins, M., Bensmaia, S.J., Washburn, S. (2001). "Vibrotactile adaptation impairs discrimination of fine, but not coarse, textures," *Somatosensory & Motor Research*, 18(4): 253-262.

Ino, S., Shimizu, S., Odagawa, T., Sato, M., Takahashi, M., Izumi, T., Ifukube, T. (1993). "A tactile display for presenting quality of materials by changing the temperature of skin surface," *Proceedings of the IEEE International Workshop on Robot and Human Communication (ROMAN '93)*, 220-224.

Jay, O., Havenith, G. (2006), "Differences in finger skin contact cooling response between an arterial occlusion and a vasodilated condition," *Journal of Applied Physiology*, 100: 1596-1601.

Johnson, K.O., Darian-Smith, I., LaMotte, C. (1973). "Peripheral neural determinants of temperature discrimination in man: a correlative study of responses to cooling the skin," *Journal of Neurophysiology*, 36: 347-370.

Johnson, K.O., Darian-Smith, I., LaMotte, C., Johnson, B., Oldfield, S. (1979). "Coding of incremental changes in skin temperature by a population of warm fibers in the monkey: correlation with intensity discrimination in man," *Journal of Neurophysiology*, 42: 1332-1353.

Jones, L.A., Berris, M. (2002). "The psychophysics of temperature perception and thermal-interface design," *Proceedings of the 10th Symposium On Haptic Interfaces For Virtual Environments & Teleoperator Systems (HAPTICS 02).*

Kalpakjian, S. (1995). *Manufacturing Engineering and Technology*. Reading, MA: Addison-Wesley.

Kenshalo, D.R. (1976). "Correlations of temperature sensitivity in man and monkey, a first approximation," *Sensory Functions of the Skin with Special Reference to Man*, Y. Zotterman, (Ed.). Oxford: Pergamon Press, 305-330.

Kenshalo, D.R., Decker, T., Hamilton, A. (1967). "Comparisons of spatial summation on the forehead, forearm, and back produced by radiant and conducted heat," *Journal of Comparative and Physiological Psychology*, 63: 510-515.

Kenshalo, D.R., Holmes, C.E., Wood, P.B. (1968). "Warm and cool thresholds as a function of rate of stimulus change," *Perception & Psychophysics*, 3: 81-84.

Kilbreath, S.L., Refshauge, K., Gandevia, S.C. (1997). "Differential control of the digits of the human hand: evidence from digital anaesthesia and weight matching," *Experimental Brain Research*, 117: 507-511.

Kron, A., Schmidt, G. (2003). "Multi-fingered tactile feedback from virtual and remote environments," *Proceedings of the IEEE Symposium on Haptic Interfaces for Virtual Environment and Teleoperator Systems*, 16-23.

Lecuyer, A., Mobuchon, P., Megard, C., Perret, J., Andriot, C., Colinot, J. (2003). "Homere: A multimodel system for visually impaired people to explore virtual environments," *Proceedings of IEEE Virtual Reality (VR '03)*, 251-258.

MacLean, K.E., Roderick, J.B. (1999). "Smart tangible displays in the everyday world: A haptic doorknob," *Proceedings of the IEEE/ASME International Conference on Advanced Intelligent Mechatronics*, 203-208.

Marks, L.E., Stevens, J.C., Tepper, S.J. (1976). "Interaction of spatial and temporal summation in the warmth sense," *Sensory Processes*, 1: 87-98.

Mascaro, S.A., Asada, H.H. (2000). "Fingernail touch sensors: spatially distributed measurement and hemodxnamic modeling," *Proceedings of the 2000 IEEE International Conference on Robotics & Automation*, San Francisco, CA.

Mascaro, S.A., Asada, H.H. (2001). "Photoplethysmograph fingernail sensors for measuring finger forces without haptic obstruction," *IEEE Transactions on Robotics and Automation*, 17(5): 698-708.

Meftah, el-M., Belingard, L., Chapman, C.E. (2000). "Relative effects of the spatial and temporal characteristics of scanned surfaces on human perception of tactile roughness using passive touch," *Experimental Brain Research*, 132(3): 351-361.

Nowak, D.A., Hermsdorfer, J., Glasauer S., Philipp, J., Meyer, L., Mai, N. (2001). "The effects of digital anaesthesia on predictive grip force adjustments during vertical movements of a grasped object," *European Journal of Neuroscience*, 14: 756-762.

Pennes, H.H. (1948). "Analysis of tissue and arterial blood temperatures in the resting forearm," *Journal of Applied Physiology*, 1: 93-122.

Rozsa, A.J., Kenshalo, D.R. (1977). "Bilateral spatial summation of cooling of symmetrical sites," *Perception & Psychophysics*, 21: 455-462.

Serina, E.R., Mote, C.D., Rempel, D. (1997). "Force response of the fingertip pulp to repeated compression – effects of loading rate, loading angle and anthropometry," *Journal of Biomechanics*, 30: 1035-1040.

Shimoga, K.B. (1993). "A survey of perceptual feedback issues in dexterous telemanipulation. I. Finger force feedback," *Virtual Reality Annual International Symposium, IEEE'93*, 263-270.

Smith, D.O., Chikayoshi, O., Kimura, C., Toshimori, K. (1991). "The distal venous anatomy of the finger," *The Journal of Hand Surgery*, 16A: 303-307.

Stevens, J.C. (1979). "Thermal intensification of touch sensation: Further extensions of the Weber phenomenon," *Sensory Processes*, 3: 240-248.

Stevens, J.C. (1982). "Temperature can sharpen tactile acuity," *Perception & Psychophysics*, 31(6): 577-580.

Stevens, J.C. (1991). "Thermal sensibility," *The Psychology of Touch*, Heller, M.A. and Schiff, W. (Eds.). Hillsdale, NJ: Lawrence Erlbaum, 61-90.

Stevens, J.C., Choo, K.C. (1998). "Temperature sensitivity of the body surface over the life span," *Somatosensory and Motor Research*, 15: 13-28.

Stevens, J.C., Hooper, J.E. (1982). "How skin and object temperature influence touch sensation," *Perception & Psychophysics*, 32(3): 282-285.

Stevens, J.C., Marks, L.E. (1971). "Spatial summation and the dynamics of warmth sensation," *Perception & Psychophysics*, 9: 391-398.

Stevens, J.C., Marks, L.E. (1979). "Spatial summation of cold," *Physiology & Behavior*, 22: 541-547.

Sutter, P.H., Iatridis, J.C., Thakor, N.V. (1989). "Response to reflected-force feedback to fingers in teleoperation," *Proceedings of NASA Conference on Space Telerobotics*, Pasadena, CA, 4: 65-74.

Tortora, G.J., Grabowski, S.R. (1993). *Principles of Anatomy and Physiology*. New York: Harper Collins.

Vega-Bermudez, F., Johnson, K., Hsiao, S.S. (1991). "Human tactile pattern recognition: active versus passive touch, velocity effects, and patterns of confusion," *Journal of Neurophysiology*, 65(3): 531-546.

Verrillo, R.T., Bolanowski, S.J., Checkosky, C.M., McGlone, F.P. (1998). "Effects of hydration on tactile sensation," *Somatosensory and Motor Research*, 15: 93-108.

Weber, E.H. (1834). *De pulsu, resorptione, auditu, et tactu*. Leipzig: Koehler.

Weber. E.H. (1846). "Der Tastinn und das Gemeingfuehl [The sense of touch and common sensibility or coenesthesia]," *Handwoerterb uch der Physiologie*, In R. Wagner (Ed.). Braunschweig: Vieweg.

Yamamoto, A., Cros, B., Hasgimoto, H., Higuchi, T. (2004). "Control of thermal tactile display based on prediction of contact temperature," *Proceedings of the IEEE International Conference on Robotics and Automation*, 1536-1541.

Yang, G., Jones, L.A., Kwon, D. (2008). "Use of simulated thermal cues for material discrimination and identification with a multi-fingered display," *Presence*, 17: 29-42.

Yovanovich, M.M. (1981). "New contact and gap conductance correlations for conforming rough surfaces," *AIAA Progress in Astronautics and Aeronautics, Spacecraft Radiative Transfer and Temperature Control*, 83: 83-95.

Zimmermann, R.J., Stevens, J.C. (1982). "Temperature-touch interactions: Is there a reverse Weber phenomenon?," *Bulletin of the Psychonomic Society*, 19(5): 269-270.